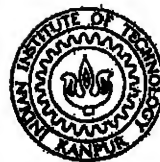


# **RELATION BETWEEN SUPERPLASTICITY AND PRIOR THERMOMECHANICAL TREATMENT IN LEAD-TIN EUTECTIC**

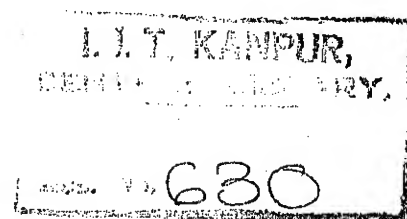
**BY  
HARISH CHANDRA CHANDAN**



**DEPARTMENT OF METALLURGICAL ENGINEERING  
INDIAN INSTITUTE OF TECHNOLOGY KANPUR  
DECEMBER 1971**

# RELATION BETWEEN SUPERPLASTICITY AND PRIOR THERMOMECHANICAL TREATMENT IN LEAD-TIN EUTECTIC

A Thesis Submitted  
In Partial Fulfilment of the Requirements  
for the Degree of  
MASTER OF TECHNOLOGY



BY  
HARISH CHANDRA CHANDAN

to the

DEPARTMENT OF METALLURGICAL ENGINEERING  
INDIAN INSTITUTE OF TECHNOLOGY KANPUR  
DECEMBER 1971



CERTIFICATE

This is to certify that this work, "RELATION BETWEEN SUPERPLASTICITY AND PRIOR THERMOMECHANICAL TREATMENT IN LEAD-TIN EUTECTIC", has been carried out by Mr. Harish Chandra Chandan under my supervision, and it has not been submitted elsewhere for a degree.

*G. S. Murty*  
( DR. G. S. MURTY )  
Assistant Professor  
Department of Metallurgical Engineering  
Indian Institute of Technology  
Kanpur, India

POST GRADUATE OFFICE  
This thesis has been approved  
for the award of the Degree of  
Master of Technology (M.Tech.)  
in accordance with the  
regulations of the Indian  
Institute of Technology Kanpur  
Dated. 20/12/21

DATED:

DETAILS OF GRADUATE COURSES CREDITED

1. MET 608 Energetics of Physical Systems
2. MET 644 Materials Science I
3. MET 652 Strengthening Mechanisms in Solids
4. MET 640 Solid State Transformations
5. MET 648 Diffusion in Solids
6. MET 652 Deformation Phenomenon I
7. MET 650 Dislocation Theory of Plastic Deformation
8. CHE 682 Nuclear Chemical Processes

GRADUATE SEMINARS CREDITED

1. Shock Hardening
2. Superplasticity
3. The Influence of Lattice Friction on Point Defect Hardening.
4. Very Early Stages in Plastic Deformation.
5. A Statistical Investigation of Microcrack Formation.

This is to certify that Mr. Harish Chandra Chanden  
has credited above listed courses and seminars.

HC Chanden  
Signature of the Student

G. S. Murthy  
( DR. G. S. MURTHY )  
Assistant Professor  
Department of Metallurgical Engineering  
Indian Institute of Technology  
Kanpur, India



ACKNOWLEDGEMENTS

I take this opportunity to thank Dr. G.S. Murty who took pains to supervise and to provide constant guidance during the work. Thanks are due to Mr.M.L.Vaidya for his useful suggestions.

Thanks are due to Mr. C.N.D. Biswas and Mr. Hari Singh Virdee who helped in testing on Instron. Thanks are also due to Mr. K.P. Mukherjee for help in metallography. Last but not the least thanks are due to Mr. Kalp Nath Tewari who typed the manuscript.

DATE:

( HARISH CHANDRA CHANDAN )

# TABLE OF CONTENTS

	Page
List of Tables and Symbols	vi
List of Figures	vii
Abstract	xi
Chapter 1 INTRODUCTION	1
1.1 Introduction	1
1.2 Review of Literature on Lead-Tin Eutectic	11
1.3 Applications	30
1.4 Aim of Present Study	32
Chapter 2 EXPERIMENTAL PROCEDURE	34
2.1 Preparation	34
2.2 Testing	35
2.3 Metallography	36
Chapter 3 RESULTS AND DISCUSSIONS	37
3.1 Initial Microstructural Observations	37
3.2 Mechanical Data	43
3.3 Microstructural Observations on Deformed Samples	46
3.4 Discussion	47
Chapter 4 CONCLUSIONS	50
Appendix 1 Materials	80
Appendix 2 Modification of Linear Intercept Method	82
Appendix 3 Precision of Linear Intercept Method	84
References	87

# LIST OF TABLES

Table 2.1	Identification of Samples	34
Table 3.1	Grain Sizes of Various Samples	39

## SYMBOLS

$\sigma$	=	True stress
$\epsilon$	=	True strain
$\dot{\epsilon}$	=	True strain rate
$T$	=	Temperature
$T_{m.p.}$	=	Melting point
$k$	=	Holtzmann constant
$\lambda$	=	Metallographic mean free path or grain size
$P$	=	Load
$V$	=	Cross-head speed

## ABBREVIATIONS

N.H.	=	Nabarro Herring
Redn.	=	Reduction
Temp.	=	Temperature

## LIST OF FIGURES

Fig.1	Schematic representation of strain rate dependence of true flow stress for Superplastic materials	..
Fig.2	Photomicrograph, As-cast, X 1110, Lamellar structure	..
Fig.3	Photomicrograph, As-cast, X 1760, Lamellar structure	..
Fig.4	Photomicrograph, As-cast, X 1110, Nonlamellar structure, $L = 1.10$ micron	..
Fig.5	Photomicrograph, As-cast, X 1760, Nonlamellar structure, $L = 1.10$ micron	..
Fig.6	Photomicrograph, A: Swaged to 0.34", % reduction in C.S. = 54%, X 1110, $L = 1.00$ micron	..
Fig.7	Photomicrograph, A: Swaged to 0.34", % reduction in C.S. = 54%, X 1760, $L = 1.00$ micron	..
Fig.8	Photomicrograph, B: Swaged to 0.26", % reduction in C.S. = 73%, X 1110, $L = 1.00$ micron	..
Fig.9	Photomicrograph, C: Swaged to 0.18", % reduction in C.S. = 87%, X 1110, $L = 0.98$ micron	..
Fig.10	Photomicrograph, D: Swaged to 0.14", % reduction in C.S. = 92%, X 1110, $L = 1.90$ micron	..
Fig.11	Photomicrograph, E: Swaged to 0.10", % reduction in C.S. = 96%, X 1110, $L = 1.70$ micron	..

Fig.12	Photomicrograph, A-1: Annealed at 120°C for 1 day, X 1110, L = 1.35 microns	..
Fig.13	Photomicrograph, B-1: Annealed at 120°C for 1 day, X 1110, L = 1.36 microns	..
Fig.14	Photomicrograph, C-1: Annealed at 120°C for 1 day, X 1110, L = 1.69 microns	..
Fig.15	Photomicrograph, D-1: Annealed at 120°C for 1 day, X 1110, L = 1.70 microns	..
Fig.16	Photomicrograph, E-1: Annealed at 120°C for 1 day, X 1110, L = 2.00 microns	..
Fig.17	Photomicrograph, A-3: Annealed at 120°C for 3 days, X 1110, L = 1.90 microns	..
Fig.18	Photomicrograph, B-3: Annealed at 120°C for 3 days, X 1110, L = 1.90 microns	..
Fig.19	Photomicrograph, C-3: Annealed at 120°C for 3 days, X 1110, L = 1.90 microns	..
Fig.20	Photomicrograph, D-3: Annealed at 120°C for 3 days, X 1110, L = 1.79 microns	..
Fig.21	Photomicrograph, E-3: Annealed at 120°C for 3 days, X 1110, L = 2.26 microns	..
Fig.22	Photomicrograph, A-7: Annealed at 120°C for 7 days, X 1110, L = 2.30 microns	..
Fig.23	Photomicrograph, B-7: Annealed at 120°C for 7 days, X 1110, L = 2.00 microns	..
Fig.24	Photomicrograph, C-7: Annealed at 120°C for 7 days, X 1110, L = 2.40 microns	..
Fig.25	Photomicrograph, D-7: Annealed at 120°C for 7 days, X 1110, L = 2.40 microns	..
Fig.26	Photomicrograph, E-7: Annealed at 120°C for 7 days, X 1110, L = 2.80 microns	..

Fig.27	Photomicrograph, SD-A: 150% Elongation, X 1110, L = 2.00 microns	..
Fig.28	Photomicrograph, SD-B: 200% Elongation, X 1110, L = 2.20 microns	..
Fig.29	Photomicrograph, SD-C: 300% Elongation, X 1110, L = 2.20 microns	..
Fig.30	Photomicrograph, SD-D: 100% Elongation, X 1110, L = 2.30 microns	..
Fig.31	Strain rate dependence of $m$ at room temperature	..
Fig.32	Effect of strain rate cycling on $m$ vs. strain rate behaviour	..
Fig.33	Effect of test temperature on $m$ vs. strain rate behaviour	..
Fig.34	Effect of annealing on $m$ vs. strain rate behaviour (54% prior reduction)	..
Fig.35	Effect of annealing on $m$ vs. strain rate behaviour (73% prior reduction)	..
Fig.36	Effect of annealing on $m$ vs. strain rate behaviour (87% prior reduction)	..
Fig.37	Effect of annealing on $m$ vs. strain rate behaviour (92% prior reduction)	..
Fig.38	Effect of annealing on $m$ vs. strain rate behaviour (96% prior reduction)	..
Fig.39	$m$ vs. strain rate behaviour of same grain sized material processed differently	..
Fig.40	Strain rate dependence of true stress at room temperature	..
Fig.41	Effect of strain rate cycling on true stress vs. strain rate behaviour	..

Fig.42	Effect of test temperature on true stress vs. strain rate behaviour (29.5% prior reduction)	..
Fig.43	Effect of annealing on true stress vs. strain rate behaviour (73% prior reduction)	..
Fig.44	Effect of annealing on true stress vs. strain rate behaviour (87% prior reduction)	..
Fig.45	Effect of annealing on true stress vs. strain rate behaviour (92% prior reduction)	..
Fig.46	Effect of annealing on true stress vs. strain rate behaviour (96% prior reduction)	..
Fig.47	True stress vs. strain rate behaviour of same grain sized material processed differently	..
Fig.48	Initial true stress and grain size vs. prior reduction	..
Fig.49	Effect of test temperature on true stress vs. % elongation behaviour (54% prior reduction)	..
Fig.50	Effect of annealing on true stress vs. % elongation behaviour (92% prior reduction)	..

### ABSTRACT

Using the widest terms of reference, Superplastic deformation can be said to be characterised by ductility under small tensile, compressive or torsional forces that is well in excess of conventional behaviour. Several investigations have been done on Superplastic behaviour of Pb-Sn eutectic. Apart from studying the general phenomenon of Superplasticity, observations have been made to delineate the effect of prior mechanical and thermal processing on Superplastic behaviour. As-cast eutectic is lamellar and is not Superplastic. Increasing prior reduction leads to a relatively equiaxed structure which has smooth interphase boundaries. Annealing produced an asymmetric structure with zig-zag interphase boundaries. The Superplastic behaviour seems to depend on nature of interphase boundary and shape of second phase particle. An equiaxed shape and smooth interphase boundary leads to better Superplastic properties. Even same grain-sized samples which were processed differently behave differently possibly because of the difference in the shape of second phase particles and nature of interphase boundary. The maximum grain size obtained by severe prior reduction and by annealing upto 7 days was 2.80 microns.



## CHAPTER 1

### 1.1 Introduction

We begin with a brief note on the historical development in this field. In 1920, Rosenhain observed that the cold-rolled Zinc: Copper: Aluminum ternary eutectic alloy 'behaved differently from ordinary crystalline materials, such as Aluminum but very similar to ... Pitch, glass etc'. A few year later Sauveur noted that an Iron bar tested in a temperature gradient exhibits regions of easy twisting at the transformation temperatures. Pearson (1934) found that a fine-grain Bismuth-Tin and Tin-Lead eutectic alloy could be extended upto 2000% in a tension test. Sauerwald (1949) reported that a number of alloys based on Aluminum and Zinc had extremely large tensile elongations. Nearly at the same time Bochvar and Sviderskaia observed the phenomenon of large extensibility, also in Al-Zn alloy. Underwood<sup>17</sup> reported a literature-survey in 1962, which covered nearly all the work done to date. Backofen, Turner and Avery<sup>18</sup> (1964) proposed and proved that Superplasticity results from a high strain-rate sensitivity of the flow stress. Their paper provided a foundation for the recent and continuing research in this field. Various metals, alloys and ceramics have been studied since 1964. Recently (1970) two more reviews<sup>14,19</sup> on the subject have appeared. Padmanabhan et.al<sup>19</sup> have listed all the metals, alloys and ceramics, that have been studied so far, along with corresponding references. A

lot of work has been done on Tin-Lead-eutectic system which is the subject of present investigation also<sup>20-25,1,15</sup>. Sn-2% Pb<sup>15</sup>, Sn-81% Pb<sup>15</sup> and Sn<sup>15</sup> have also been studied.

A superplastic material (metal, alloy or a ceramic) flows with the fluid-like character of hot polymers and glasses. In solid crystalline materials this is a relatively rare phenomenon and only in the last six years has it been widely demonstrated. At the present time Superplasticity is most commonly associated with exceptionally large elongations in metals but is not necessarily restricted to such cases and no particular mechanism of deformation is inferred by applying the name 'Superplastic'. Using the widest terms of reference, Superplastic deformation can be said to be characterised by ductility under small tensile, compressive or torsional forces that is well in excess of conventional behaviour.

Superplastic materials can broadly be divided into two groups :

(1) Structural Superplasticity: is exhibited by those materials in which a characteristic structural condition exists, e.g., a stable, ultra-fine grain size of the order of a few microns.

(2) Environmental Superplasticity: is exhibited by those materials for which special testing conditions are necessary, e.g., temperature cycling under a small applied stress. This cycling induces repeated phase transformation as in Iron.

In both groups, it is now generally agreed that the extensive elongation can be correlated with a high strain-rate

sensitivity of flow-stress<sup>26-28,18</sup>. This characteristic is described by a parameter  $m$  defined by :

$$m = \frac{\partial \log \sigma}{\partial \log \dot{\epsilon}} \quad \dots \quad (1)$$

where  $\sigma$  = Applied true stress  
 $\dot{\epsilon}$  = True strain rate.

In general, the magnitude of  $m$  identifies a Superplastic material irrespective of the mode of straining and the origin of Superplastic behaviour. The materials exhibiting Structural Superplasticity have  $m$  in the range 0.3 - 0.8, while the materials exhibiting Environmental Superplasticity have  $m \cong 1$ . In conventional materials  $m$  is less than 0.3. In glass,  $m = 1$  and this material exhibits Newtonian-viscous behaviour. Materials which show serrated yielding have negative  $m$ .

The superplastic elongation is different from normal elongation. This can be explained as follows. A normal ductile material when stretched by a tensile force can deform uniformly only when stable flow occurs. The flow, at temperatures less than about  $T_m/2$  ( $T_m$  is melting point of material), is stabilised by strain hardening effects. The limit of stable flow is marked by the onset of geometrical instability or necking which occurs when the material has exhausted its capacity for strain hardening. For further stable extension the material must be unloaded and then annealed, thus restoring the ability to strain-harden again on applying the load. This is the behaviour of normal material. The Superplastic material

deforms differently. It does not strain-harden. In this case, the stable flow is not due to the strain-hardening effect but is due to high strain-rate-sensitivity of flow stress. Mathematically, for a normal ductile material we have, at test temperature  $T < T_m/2$ ,

$$\sigma = C \epsilon^n \quad \dots (2)$$

where  $\sigma$  = True stress  
 $\epsilon$  = True strain  
 $C$  = Strength coefficient  
 $n$  = Strain-hardening-exponent.

The value of  $n$  is generally less than 0.3 which means that the stable flow or uniform elongation does not exceed 30% elongation because it can be shown both theoretically and experimentally that

$$\epsilon_{\text{necking}} = n$$

At test temperature  $T > T_m/2$ , the stability of plastic deformation is due to high strain-rate-sensitivity of flow stress. Mathematically,

$$\sigma = K(\dot{\epsilon})^m \quad \dots (3)$$

where  $K$  = constant for given testing conditions and  
 $m$  is a material parameter.  
 $\dot{\epsilon}$  = Strain rate.

The stability of plastic deformation when both strain-hardening and strain-rate effects need to be considered, has been examined by Rossard<sup>39</sup>, Hart<sup>28</sup> and Campbell<sup>40</sup>. In such a case,

$$\sigma = (K') (\epsilon)^n (\dot{\epsilon})^m \quad \dots \quad (4)$$

where  $K = A$  constant embracing  $C$  and  $K$  of eqn.(2)  
and eqn.(3).

It was shown that deformation is stable provided,

$$\frac{n}{\epsilon} + m \geq 1$$

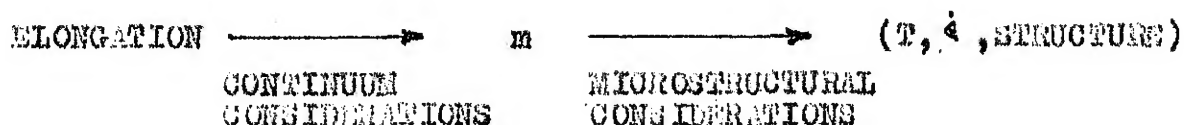
This criterion is valid both for normal and superplastic materials. For normal materials there is no strain-rate dependence ( $m = 0$ ), so condition of stable flow is,  $\frac{n}{\epsilon} \geq 1$  — the end point coming when  $n = \epsilon$ , after which necking begins. For viscous materials, ( $n = 0$ ) the condition of stable flow<sup>41</sup> is  $m \geq 1$ . These were ideal and extreme cases. Furthermore, if we consider the case where  $n$  is small and we get eqn.(3), then the rate at which the strain gradients increase, is expected to be low for  $m \geq 0.5$  even though a state of plastic instability exists<sup>39,40</sup>. This is the case of an actual Superplastic material. This is consistent with the formation of a series of diffuse necks in Superplastic elongation. The apparently uniform Superplastic elongation which, in fact, is rather a very much extended version of a neck or a series of diffused necks, was explained by Backofen et.al.<sup>18</sup> on a phenomenological basis. Using constancy of volume in plastic deformation, we get :

$$\begin{aligned} \dot{\epsilon} &= - \frac{1}{A} \frac{dA}{dt} \\ \sigma &= \frac{L}{A} \end{aligned} \quad \dots \quad (5)$$

where  $A =$  Cross-sectional area

30. M. Rieffel, 'A characterisation of commutative group algebras and measure algebras', *Trans. Amer. Math. Soc.*, 116(65) 32-64.
31. M. Rieffel, 'Induced Banach representations of Banach algebras and locally compact groups', *J. of Functional Analysis*, 1(1967) 443-491.
32. M. Rieffel, 'Multipliers and tensor products of  $L^p$ -spaces of locally compact groups', *Studia Mathematica*, 33(1969) 71-82.
33. H.P. Rosenthal, 'Projections onto translation invariant subspaces of  $L^p(G)$ ', *Mem. Am. Math. Soc. No. 63*, 1966.
34. W. Rudin, 'Fourier Analysis on groups', *Interscience Tracts in Pure and appl. Math. no. 12*, Interscience, New York, 1962.
35. W. Rudin, 'Functional Analysis', *Mc-Graw Hill Inc.*, 1973.
36. H.H. Schaefer, 'Topological Vector Spaces', *Mc-Millan*, New York, 1966.
37. R. Schatten, 'A theory of cross-spaces', *Annals of Mathematics Studies no. 26*, Princeton Univ. Press, 1950.
38. I. Singer, 'Linear functionals on spaces of continuous mappings of a compact Hausdorff space into a Banach space', *Rev. Math. Pures. Appl.* 2(1957) 309-315.
39. J.L. Taylor, 'Measure Algebras' *Regional Conference Series in Math. no. 16*, Conference Board of Mathematical Sciences, 1973.
40. J. Tomiyama, 'Tensor products of commutative Banach algebras', *Tohoku Math. J.* 12(1960) 147-154.
41. J.J. Uhl Jr., 'The range of a vector-valued measure', *Proc. Amer. Math. Soc.* 23(1969) 158-163.
42. A. Weil, 'L'integration dans les groupes topologiques et ses applications', *Hermann*, Paris, 1951.
43. A.J. White, 'Ordered Banach algebras', *Journal London Math. Soc., Ser. 2*, 11 (1975) 175-178.

A good agreement was found between this equation and experimental data from Lee and Backofen<sup>26</sup>. It was found that the elongation strongly depends upon  $m$ . It was also found that 200% elongation is possible with  $m$  as low as 0.3. The relationship between elongation and microstructure can be schematically illustrated as



That is, elongation is related to  $m$  through continuum considerations. The index  $m$  is related to microstructure and the temperature and strain rate through metallurgical, property-structure considerations.

With this general background of Superplasticity (both structural and environmental) we now take up Structural Superplasticity which is relevant to the present investigation on Tin-Lead eutectic.

## 1.2 Structural Superplasticity

This has been observed in a large range of two phase alloys, many of which are eutectic or eutectoid. Most superplastic materials exhibit a sigmoidal variation of  $\log \epsilon$  vs.  $\log \dot{\epsilon}$ . The slope of this curve is  $m$ . The second region has  $m \geq 0.3$  and is Superplastic. First and third regions have  $m \leq 0.1$  and correspond to conventional plasticity. Alloys of Lead-Tin<sup>1,15</sup>, Tin-Bismuth<sup>44</sup> show all three regions. A



large number of experiments have been carried in second region but they have not produced data which define a unique rate-controlling mechanism. Nevertheless, it has been clearly demonstrated that three important interdependent criteria must be satisfied if superplastic behaviour is to occur. They are:

(1) The material must have a fine ( $< 10$  micron), equiaxed grain size which remains stable at the temperature of deformation. The simplest way of obtaining the required stable grain structure is by producing a two-phase mixture in which phases are present in approximately equal proportions. In general, such alloys are of eutectic or eutectoid composition. The As-cast material is heavily hot-worked to produce an intimate mixture of the two phases such that both phases have fine grain sizes. In some cases, Spinodal decomposition also produces the correct structure<sup>45</sup> and two-phase mixtures in which one phase pins the grain boundaries of the other are also effective in stabilising the grain size so as to produce Superplasticity<sup>46-50</sup>. If one of the phases has a larger grain size<sup>3</sup> (e.g. an annealed eutectic alloy), or if grain growth occurs during testing<sup>15,8,51</sup> or if the grains are not equiaxed<sup>1,44,45,3</sup> the ability to show Superplasticity is lost.

(2) The strain-rate-sensitivity index  $m$  of the material should be high ( $m > 0.3$ ) compared with conventional materials ( $m \approx 0.1$ ). The value of  $m$  depends upon grain size, temperature of deformation and strain rate. In general,  $m$  increases with decreasing grain size or increasing temperature but goes through a maximum with increasing strain rate. Maximum elongations are



frequently obtained under conditions of maximum  $n$ , and it has been pointed out<sup>52</sup> that there is a general relationship between the value of  $n$  and the elongation to fracture. However, there is considerable scatter and detailed interpretation of the relationship is not possible at present.

(3) There is some indication that the diffusion rates in both phases of duplex alloys should be similar at the deformation-temperature if the superplastic elongation is to take place.

In superplastic alloys satisfying the above 3 criteria, it has been found that an activation energy  $Q$  for the deformation process can be determined from the experimental relationship. At constant stress and grain size,

$$\dot{\epsilon}_{\sigma, L} \propto \exp(-Q/kT) \quad \dots \quad (8)$$

where  $k$  = Boltzman constant

$\dot{\epsilon}$  = strain rate

$T$  = Temperature

and  $Q$  = Activation energy

$L$  refers to grain size and  $\sigma$  to stress.

The activation energy is largely independent of grain size but its meaning is not at all clear since it is of the order of magnitude of the activation energy for volume diffusion in Fe-Ni-Cr and Ti alloys<sup>19</sup> and of the activation energy for Grain-boundary-diffusion for Sn, Pb and Zn alloys. Nevertheless it is apparent that diffusional processes are of considerable importance in superplastic flow. This

view is reinforced by recent observation<sup>58</sup> that alloying elements which increased atomic mobility also enhanced Superplastic behaviour. The strain rate corresponding to a given flow stress and temperature, has been shown to vary with grain size,  $L$ , as:

$$\dot{\epsilon} \propto \frac{1}{L^a} \quad \dots (9)$$

The exponent 'a' has been given as<sup>19</sup> 2 and 3. In these circumstances it would seem justifiable to accept the views of Jones and Johnson<sup>69</sup> and Packer and Sherby<sup>67</sup> that the exponent can only be considered to lie within the above values as limits.

The variation in flow-stress with grain size at constant strain rate has been reported as :

$$\sigma \propto L^b, \quad 0.7 < b < 1.2 \quad (10)$$

Combining eqns.(8), (9) and (10) we get

$$\dot{\epsilon} = \text{Const.} \frac{(\sigma)^c}{L^a} \exp(-Q/kT) \quad \dots (11)$$

where

$$c = a/b$$

and

$$1.6 \leq c \leq 4.2$$

Comparing (11) with (3) we see that,

$$c \sim 1/m, \quad 0.3 < m < 0.7$$

With this general background of Superplasticity, we now focus our attention on Lead-Tin eutectic system.

## 1.2 Review of Literature on Lead-Tin Eutectic

Pearson made some observations on Lead-Tin eutectic system. He tested extruded samples in tension and observed microstructures also. He also studied effect of annealing on elongation.

The mean grain size or metallographic mean free path,  $L$ , was measured to be 1.27 microns. The room temperature elongation of this material was greater than 1100% at an initial true strain rate of  $\approx 10^{-2} \text{ sec.}^{-1}$  (It was a constant cross-head speed test in which strain rate goes on decreasing as the gage length elongates more and more). After annealing at 100°C for 5 hours the grain dimension was increased to 50 to 100%, and this led to a 47% drop in elongation. From the reported data, calculation of  $m$  values shows that above annealing treatment led to a drop in  $m$  value<sup>1</sup> from 0.5 to 0.3. At high strain rates, or if the material was in As-cast condition, only normal ductility was observed. An equiaxed granular structure was observed on an initially flat surface, while rapid straining produced elongated grains.

It was concluded that the ability for stretching decreased with annealing time to increase grain size, thus emphasizing the requirement of ultra-fine grain size for observing Superplasticity. He attributed the large elongation in the extruded alloy to the persistence of extremely small grains to a temperature sufficiently high for intergranular flow.

For nearly three decades there was no further work in this field, when Avery and Backofen<sup>1</sup> took this up. They employed two methods of preparing the Lead-Tin eutectic. One was patterned after Pearson and consisted of extruding the cast Pb-Sn eutectic and then annealing to produce a range of grain sizes (grain size equals metallographic mean free path). Then they determined the strain rate dependence of  $n$  and flow stress. Elongation tests were conducted at constant cross-head speed. The other method of preparation consisted of pack rolling sheets of pure Lead and pure Tin built up in alternate layers. For metallography, surface was electro-polished and etched<sup>1</sup>. The metallographic mean free path,  $L$ , was determined by Linear Intercept method.

Before going into results and conclusions it would be better to consider the proposed model for Superplastic deformation first. They suggested that there are two competitive processes for high temperature deformation (For Superplastic deformation, Test Temp.  $> T_m/2$ , where  $T_m$  is melting point of the material) at all strain rates. They are :

- (a) Climb regulated movement of dislocations across grains and
- (b) Vacancy migration within the grains.

Mathematically, Superplastic deformation can be described by :

$$\dot{\epsilon} = A \sinh B \epsilon + C \quad \dots (12)$$

(a)
(b)

where,  $A$ ,  $B$  and  $C$  vary with  $\dot{\epsilon}$  and  $T$ .

$A = A' \rho D$ ,  $\rho$  being the density of moving dislocations and  $D$  is the diffusion coefficient, and  $A'$  is a factor incorporating the burgers vector and interjog distance.

$B = \frac{V^*}{kT}$ ,  $V^*$  being the activation volume.

$C \approx \frac{1}{\eta} \approx \frac{\alpha V D_s}{L^2 kT}$ ,  $\eta$  being Nabarro-Herring (N-H) viscosity,  $L$  being the length of the vacancy diffusion path or metallographic mean free path, and  $D_s$  being self diffusion coefficient.  $\alpha \approx 10$

At low strain-rates N-H creep or vacancy diffusion within the grains (b) predominates while at higher strain-rates climb-regulated movement of dislocations across grains is the dominant mechanism. At all strain-rates there is a competition between (a) and (b). At some strain-rate depending upon the value of there is equal contribution from the two components. This strain rate is called transition strain rate as at this strain rate there is transition from one dominant mode to other dominant mode. If  $\eta$  is high (i.e., N-H viscosity is high for the material) the transition strain rate,  $\dot{\epsilon}_t$ , occurs at a relatively lower value of strain rate as compared with the case when  $\eta$  is low. Superplastic materials have a low value of  $\eta$  (or high  $C$ ) because in these high  $m$  condition is observed at higher strain rates ( $10^{-1}$ /sec.). Conventional materials have a high value of  $\eta$  (or low  $C$ ) because as strain rate increases from  $10^{-7}$ /sec.  $m$  value begins to decrease. From the equation (12)

for Superplastic flow,  $\dot{\epsilon}_t \propto D/L^2$ . This means that the most effective means of shifting  $\dot{\epsilon}_t$  to higher strain rates (i.e. observing Superplasticity) is refinement of grain size. Thus this model predicts two things:

(i) At low strain rates,  $m \rightarrow 1$ , i.e., Newtonian viscosity.

$$(ii) (\dot{\epsilon})_{\infty} \propto \frac{D}{L^2}$$

They ruled out grain-boundary shear as a mechanism for superplastic deformation. The argument is as follows. If this were to occur intercrystalline cracking and limited ductility ought to be observed. Moreover, Superplastic materials may contain a high density of interphase boundaries (of limited mobility) while undergoing enormous strains before fracture; the rate of shear near grain boundaries cannot be much different from the rate within the grains.

Now, we come to results. In the As-cast material  $m$  was consistently low ( $= 0.1$ ) for all strain rates and tensile fracture involved necking plus extensive formation of internal voids. However, the microstructure of the As-cast material was fine. Even after aging for 4 weeks at room temperature the mean free path was 0.97 microns. The extruded samples exhibited Superplasticity. After annealing the grain size increased and percentage elongation went down. Elongation tests at constant cross-head speed gave the information that as elongation increases the  $m$  value increases. In metallography there was problem of etching to reveal grain boundaries simultaneously in Pb- and Sn-rich phases. Metallographic examination after testing produced



no evidence of intergranular voids in high  $m$  material. Voids were apparent, however, in samples which were annealed for 72 hours at  $150^{\circ}\text{C}$ , though it showed a peak  $m = 0.45$ . Pack rolling of alternate layers of Sn and Pb produced more or less lamellar structure in which grains of both phases would be limited in size by the lamella thickness. The minimum  $L$  obtained was 1 micron.

It was concluded that  $\dot{\epsilon}_t \propto 1/L^2$  is obeyed. However, As-cast Lead-Tin eutectic was not Superplastic in spite of the fine structure. It was found that the particles of Lead-rich phase were rod shaped and length of rods was 10-20  $L$ . They suggested that for strongly asymmetric grain shapes such as these, the long dimension should be rate controlling. If it is so the observation in As-cast material is consistent with  $\dot{\epsilon}_t \propto 1/L^2$ . Through extrusion the initial structure is replaced by one that is no finer in terms of  $L$  but is much more nearly equiaxed. The absence of intergranular voids in high  $m$  confirms the lack of contribution from grain boundary shear in Superplastic deformation.

In 1966, Martin and Backofen<sup>24</sup> reported yet another method of getting fine grain size. They prepared Lead-Tin composites by electrodeposition in alternate layers of 0.5 to 5 microns thickness. This method allowed close control of the grain size while introducing resistance to grain growth. They confirmed Avery and Backofen's earlier finding that  $\dot{\epsilon}_t \propto 1/L^2$ .

i.e., increasingly fine microstructure enables a material to behave Superplastically to higher levels of strain rate. However, they pointed out that small grain size is only a necessary condition for Superplasticity. They reported that at  $\dot{\epsilon} < \dot{\epsilon}_t$ ,  $\sigma \propto L^a$ , where  $a = 0.5 - 0.9$  instead of  $a = 2$  as reported by Avery and Backofen<sup>1</sup>. Therefore, grain boundary shear should be the rate controlling mechanism at  $\dot{\epsilon} < \dot{\epsilon}_t$  instead of vacancy diffusion within the grains as suggested by Avery and Backofen<sup>1</sup> (which gives  $a = 2$ ). The effect of annealing after plating was much like that of coarsening the grain size, even though the grain size was not changed. The response to annealing was related to the precipitation from the supersaturated Lead-rich phase that is developed by heating the mixture of pure components.

In 1967, Cline and Alden<sup>15</sup> reported a study on Lead-Tin eutectic covering a larger range of strain rates, compositions, temperatures and microstructure. They also investigated the question why As-cast structure does not exhibit Superplastic behaviour although it appears to have a fine microstructure. They used materials of 99.99% purity and ingots were cast in graphite molds in Argon. They arrived at same grain size through different thermomechanical treatments. To observe the grain size in samples in which grain growth was occurring at room temperature, a diamond knife microtome was used. An electropolish was used as suggested by Avery and Backofen<sup>1</sup>. The grain size is specified by the mean intercept length.



The microstructure of the eutectic alloy showed uniformly distributed, equiaxed grains of Tin and Lead. The grain size was,  $L = 2$  microns. The micrograph of a unidirectionally solidified (6 inches/hour) eutectic apparently showed a fine microstructure which, however, on examination with polarised light clearly showed that the Tin grains were very large and have fine Lead particles dispersed in them. The deformed and annealed sample ( $170^{\circ}\text{C}$ , 1 hour) showed a grain size of 10 microns. Deformation of this annealed sample revealed grain boundaries and interphase boundaries of the equiaxed structure. The continuous scratches on electropolished surface showed discontinuities at the boundaries after deformation.

The  $\log \sigma - \log \dot{\epsilon}$  curve was S-shaped or sigmoidal. Widely different  $\log \sigma$  vs  $\log \dot{\epsilon}$  curves were found for different compositions. A comparison of % elongation for various compositions showed that % elongation was maximum for eutectic composition. The value of  $m$  at low strain rates is 0.3, goes through a maximum of about 0.5 and approaches 0.1 at high strain rates. With increasing temperature the flow curve shifts to higher strain rates without a significant change in shape. From a plot of  $\log \dot{\epsilon}$  vs.  $1/T$  at constant stress, the apparent activation energy is  $0.5 \pm 0.1$  e.v., whereas the activation energy for self diffusion is 1 e.v. for both pure Lead and pure Tin. The As-cast eutectic does not exhibit large elongation

or high  $n$  value. The  $\log \dot{\epsilon} - \log \epsilon$  curve is not sigmoidal but is a straight line for As-cast eutectic and is similar to large-grain pure metals. At all strain rates  $n$  value is low for As-cast eutectic.

They conclude that dilute alloys and even pure metals can exhibit high  $n$  at relatively high strain rates if the grains are small and remain small during the test. The mechanism by which a metal becomes Superplastic depends on grain size but does not require the presence of two phases or alloying elements in solid solution; nor does it depend upon a special property of a eutectic as, for example, its low melting point. The important role of composition is its effect on grain growth. The greater the volume of second phase, the lower the rate of grain growth because of the relative immobility of interphase boundaries. They emphasized that high peak  $n$  alone is not sufficient for large elongations. The initial fine grain size which leads to high  $n$  should remain fine during Superplastic deformation. For example, the eutectic Lead-Tin alloy showed maximum % elongation because its grain size was comparatively more stable during Superplastic deformation. In other non-eutectic compositions grain growth occurs by Superplastic deformation. This grain growth during Superplastic deformation reduces the  $n$  value during straining. For the same reason pure Tin is not Superplastic although it can exhibit a high peak value of  $n$ .

They concluded that the dominant mode of deformation at low strain rates in the Superplastic region is grain boundary sliding. This conclusion was arrived at from the metallographic evidence that the boundary regions were clearly revealed by straining and there were scratch-offsets at both interphase boundaries and Tin phase boundaries which is the majority phase (71% by volume). The onset of grain boundary sliding causes a rapid decrease in flow stress. They point out that it is not necessary that grain boundary sliding should account for all the deformation in this strain rate range but only that it acts to modify the deformation process so that the flow stress drops rapidly. In this sense, grain boundary sliding is not unique, and other mechanisms yet unidentified could have a similar mechanical effect. Using the information from Hart's<sup>28</sup> study of mechanical behaviour of Newtonian viscous grain boundaries dispersed in a non-Newtonian medium, they suggest that if Grain boundary sliding is Newtonian-viscous, then at very low strain rates, the grain boundary regions may be fully relaxed and the flow stress determined by the accommodation process. In this case the rate sensitivity index  $n$  would not necessarily approach 1 at low strain rates. Thus, this removes the objection with Avery and Bockofen's<sup>1</sup> model based on vacancy diffusion within the grains or N-H diffusional creep at low strain rates. At high strain rates, they suggested, slip is predominant mode of deformation.

In 1967, Packer and Sherby<sup>67</sup> suggested that Avery and Backofen's<sup>1</sup> equation (12) could not explain the Superplastic behaviour of Pb-Sn eutectic system quantitatively though it could qualitatively explain the Superplastic behaviour of Pb-Sn eutectic and other eutectic alloy systems. The predominance of Nabarro-Herring creep or vacancy migration within the grains at low strain rates which was proposed by Avery and Backofen<sup>1</sup> is not substantiated by later workers<sup>15</sup>. Packer and Sherby made a computer program and using least-square curve-fitting technique proposed following equation which correctly describes the Superplastic behaviour of Lead-Tin eutectic

$$\dot{\epsilon} = \frac{A'\bar{\alpha}^2}{L^3} + B'(\bar{\alpha})^2 \sinh \beta'(\bar{\alpha})^{2.5}$$

where,  $A'$ ,  $B'$  and  $\beta'$  are constants at a given temperature. This equation has a composite nature and is similar to Avery and Backofen's<sup>1</sup> earlier equation for Superplastic deformation. The inverse grain size square dependence of  $\dot{\epsilon}$  is now changed to inverse grain size cube dependence by Packer and Sherby. The first term is believed to account for a recrystallisation or grain boundary migration process, but no exact physical model was proposed to account for this. The second term was written with the help of Weertman's<sup>71</sup> theoretical expression which describes the creep behaviour of metals at high strain rates when dislocation climb is

rate-controlling. No modification of Weertman's expression, which was derived for metals, was done to account for the alloy nature of the system.

In 1968, Zehr and Backofen reported<sup>59</sup> a study on commercially pure Sn-Pb alloys of various compositions (14, 39, 62 and 80 wt% Tin). Air melting was done. Preliminary experiments indicated no significant difference in the behaviour of material made by vacuum melting and hydrogen purging of heats of high purity components. Each ingot was given a 28:1 area reduction at room temperature and then stored at -40°C until test. Use of higher reductions upto 256:1 had negligible effect on the behaviour. For metallography, mechanical polishing was done and then the sample was electropolished<sup>59</sup> to remove the abraded surface layer. Then etching was done with an etchant<sup>59</sup> which was different from that used by earlier workers<sup>1</sup>. Grain size refers to metallographic mean free path and was determined by linear intercept method. The number of intersections was greater than 20 which gives an uncertainty in  $L$   $\pm 10\%$ . No discrimination was made between grain and phase boundaries in finding  $L$  (considering the phases separately it was found  $\frac{L_{Sn}}{L_{Pb}} = 1.3$  in the extruded eutectic). Electron microscopy was done. Grain size after extrusion was increased by annealing in air at 160°C. In the Pb-Sn eutectic, Tin phase occupies nearly 71% volume and appears as continuous, relatively smooth matrix surrounding the roughened looking Pb-rich phase. The extruded eutectic gave a grain size of 2 microns.

They found that for Pb-Sn eutectic alloy the mechanism for superplastic deformation is one of non-Newtonian grain boundary sliding and diffusional (Newtonian) creep acting in parallel with each other and in series with more common non-Newtonian slip creep. The basis of their argument was both mechanical and metallographic evidence. The experimental relationship can be reproduced by semiempirical procedures that it suggests, and there is structural evidence as well from replica electron microscopy of the separate processes. From surface observations they conjectured the presence of diffusional creep. This was not substantiated as no internal indications of diffusional creep could be observed. This conflict becomes only apparent, however, once it is recognised that observed grain growth could be accompanied by a grain-shape relaxation and thus mask grain elongation from diffusional straining. The variation of composition disclosed no changes in the basic behaviour pattern. There was, however, an indirect evidence that grain boundary sliding was easiest in the 50 - 50 volume fraction alloy, suggesting that inter-phase boundary is a favoured site for that process.

Another work was reported in 1968. Avery and Stuart<sup>22</sup> studied the role of surfaces in Superplasticity. They studied a near eutectic Lead-Tin alloy (40% Pb, 60% Sn) which was air melted under charcoal. The starting materials were straits Tin (99.8%) and chemical Lead (99.9%). The alloy was poured at



260°C into a bottom-gated brass chill mold, yielding, after removal a slab-type casting. The ingots were machined slightly and were subsequently rolled in 10% passes at room temperature to a total reduction in area of 93.3%. Strip tensile specimens had gage section either parallel or perpendicular to the rolling direction. The thickness was constant to  $\pm 0.0005$ " along each gage length. Specimens were annealed for three hours at room temperature, others for 7.5, 30 and 52 hours at 150°C. Grain sizes or metallographic mean free paths were 1.5, 3.25, 3.52 and 3.65 microns respectively. All material was stored at 47°C prior to testing. The test temperatures varied only by  $\pm 0.5^\circ\text{C}$  during any single test. Such close temperature control was necessary because normal room temperature variations resulted in considerable scatter :

$$\left. \frac{1}{\sigma} \frac{\partial \sigma}{\partial T} \right|_{\epsilon} \times 100 = 3\% \text{ per } ^\circ\text{C}$$

Test temperatures ranged from  $-50^\circ\text{C}$  to  $+50^\circ\text{C}$ . Strain was measured with an extensometer affixed to the grips rather than to the specimen itself, since direct attachment caused damage to and distortion of the sample. Load versus extension was plotted on an X-Y recorder. About 100 tests were done.

The log - log curves were sigmoidal. The  $n$  vs. curves for 1.5 microns grain size material for various testing temperatures were similar to one another, being

displaced with decreasing temperature to lower and lower values of strain rate. The curves all show a characteristic increase in  $m$  with decreasing strain rate, rising from  $m = 0.15$  to a maximum near  $m = 0.5$ , followed by a gradual decrease. The peak  $m$  values are slightly higher in the transverse direction, and show less drop at low strain rates in the transverse direction.  $\log \sigma$  vs.  $\log \dot{\epsilon}$  plots show a slope of 2 in the Superplastic region (or  $\sigma \propto \dot{\epsilon}^2$ ). As the strain rate increases and the temperature decreases, the slope decreases, with the stress eventually becoming essentially independent of grain size. The stress in the transverse direction is always lower than that in the rolling direction, particularly at low strain rates. The grain size was equiaxed within the limits of experimental error, and would not appear to account for this anisotropy. Activation energy plots of  $\dot{\epsilon}_0$  vs.  $1/T$  show considerable curvature,  $Q$  increasing with  $\sigma$  and decreasing with  $T$  over the range 11-18 Kcal.

They looked into various mechanisms proposed till then, and suggested that ideally the mechanism should have a physical model, should be able to predict quantitatively, should explain the very strong sensitivity of Superplastic behaviour to grain size, should be able to account for  $m$  having a maximum and then falling off at both higher and lower strain rates, and it should account for the observed anisotropy. Towards this end they proposed a model which



is an extension of diffusional climb model. It includes a back-stress term  $\alpha_0$ . The creep equation for the material over a wide range of strain rates was proposed to be :

$$\dot{\epsilon} = \frac{150 \Omega D_{g.b.} w \alpha (\alpha - \alpha_0)}{k T L^3} + B \sinh \frac{V^* (\alpha - \alpha_0)}{k T}$$

where,  $\Omega$  = Atomic volume

$D_{g.b.}$  = Grain boundary diffusion constant.

$w$  = Grain boundary width (of the order of a few atoms length)

$B$  = A constant

$V^*$  = Activation volume.

The first term is derived from Coble model<sup>31</sup> for grain boundary diffusion. The second term is to account for climb regulated movement of dislocations. The high rate sensitivity at intermediate strain rates reflects a substantial contribution of grain boundary diffusional creep. At high strain rates, dislocation climb is the predominant term and at low strain rates the  $\alpha_0$  term becomes dominant, with a consequent low  $m$ .

They could not positively identify the origin of  $\alpha_0$ . They proposed that it arises from a mechanical fibering, producing a composite strengthening in the direction. They were not able to obtain any clear metallographic evidence for these fibers. The back stress was defined so that,  
 $(\alpha - \alpha_0) = K \dot{\epsilon}^m$ , where  $m$  makes a smooth transition from 1

at  $\dot{\epsilon} \ll \dot{\epsilon}_p$  (strain rate at peak  $m$ ) to  $m = 0.15$  at  $\dot{\epsilon} \gg \dot{\epsilon}_p$

For Lead-Tin,  $\infty$  fits the equation

$$\dot{\epsilon} = C \exp(-Q/RT) \exp\left(\frac{V^* \infty}{kT}\right)$$

where,  $Q = 19$  Kcal.

$$V^* = 10^{-20} \text{ cm}^3.$$

The constant  $C$  increases with impurity level and is considerably greater in the rolling than in the transverse direction. They also concluded that the rate of neck growth depends directly on surface irregularities and inversely on  $m$ . The high  $m$  (0.35 - 0.9) characteristic of Superplastic materials is in turn related to an inverse power function of the grain size. They made a remark that none of mechanisms proposed till then was adequate to describe completely the  $\infty - \dot{\epsilon} - L - T$  behaviour, although they all accounted for various aspects of it.

In 1969, Aldrich and Avery<sup>29</sup> reported a study on cyclic straining of the Lead-Tin eutectic. The eutectic Pb-Sn alloy exhibited Superplastic behaviour in Alternating uniaxial fatigue similar to that reported in tension. Their work indicated that at low strain amplitudes the rate controlling mechanism for Superplastic behaviour is grain boundary sliding. With increasing strain amplitudes the rate controlling mechanism switches to Coble grain boundary diffusion. With increasing temperatures the transition from grain boundary sliding to grain boundary diffusion as

a rate controlling mechanism occurs at lower strain amplitudes. They noted that the fatigue life of Superplastic alloys was strongly dependent on the strain rate. They noted that in the region of high  $n$  values the fatigue resistance is enhanced because of increased difficulty for crack nucleation. They pointed out that Superplastic behaviour is not the result of a unique mechanism, but rather the mechanism varies as a result of the conditions imposed on the system. They suggested that high angle boundaries which act as effective sources and sinks for vacancies are an important prerequisite for Superplastic behaviour.

Another study of Lead-Tin eutectic<sup>84</sup> was reported by Rawal in 1969. Materials used were of commercial purity. He found that Superplastic behaviour was observed at relatively low strain rates ( $\dot{\epsilon} = 3 \times 10^{-3}/\text{min.}$ ) as compared with the strain rates generally used for different forming operations. This was attributed to the large grain size (100 microns for As-Cast eutectic). He found that by increasing the amount of hot work it was possible to refine the grain size considerably. He found that the grain size was unstable during Superplastic deformation. There was both mechanical and microstructural evidence for this. He concluded that grain boundary sliding associated with continuous recrystallisation as the accommodation process was the

mechanism of Superplastic deformation. He also found that the flow stress dependence on the grain size at high temperature was different from the one at low temperature.

In 1970, Burton<sup>79</sup> reported a study of low strain rate behaviour of Lead-Tin eutectic. Using a conventional creep testing machine he found that  $\log \dot{\epsilon}$  vs  $\log \epsilon$  plots were sigmoidal. He found that  $L = 2$  microns in rolled samples of Lead-Tin eutectic, but coarsening occurred quite rapidly at room temperature. The stable structure was only achieved after holding for two months at room temperature when the mean free path has increased to 6 microns. This appeared to be an upper limit for coarsening since no further increase was detectable over a long period of time. Creep results obtained at room temperature for these stabilised 6 microns specimen were plotted in the conventional manner ( $\log \dot{\epsilon}$  vs.  $\log \epsilon$ ) and sigmoidal curve was obtained. The peak  $n$  occurred at  $\dot{\epsilon} = 10^{-8}$ /sec. which is lower than previous studies. The occurrence of peak  $n$  at low strain rates was ascribed to large grain size. Elongation tests at a strain rate corresponding to peak  $n$  ( $10^{-8}$ /sec.) were not conducted as they were very time consuming (i.e., at  $10^{-8}$ /sec. for 100% elongation we need 3 years). He suggested the existence of a threshold stress  $\sigma_0$ . No physical explanation of the threshold stress was given. However, it was pointed out that a similar onset stress was observed for grain boundary sliding in bicrystals of Al containing a dispersion of Fe

particles. He pointed out that if a threshold stress exists, the concept of  $n$  can be misleading. He suggested that in case of Pb-Sn eutectic the deformation behaviour should not be classified in terms of  $n$  values but should be considered in the following stress ranges :

- (i) Below  $\sigma_0$  no deformation occurs.
- (ii) At intermediate stress level 'true' Superplasticity occurs probably by a grain boundary sliding process.
- (iii) At higher stress levels usually recovery creep processes operate.

He emphasised that the tests should be conducted after stabilizing the grain size. Otherwise, grain coarsening during testing leads to systematic errors if  $\sigma$ - $\dot{\epsilon}$  relationship is investigated using stress increment or decrement tests on a single specimen. Since strain rate decreases with increasing grain size the strain rate at which subsequent stress levels will be less than expected, thus, giving rise to over- and underestimates of  $n$  respectively. He pointed out that similar errors can arise if strain rate increment and decrement tests are performed.

The most recent (1970) report available on Lead-Tin eutectic is that of Cutler and Edington (to be published, see Reference 19). By optical metallography they found that in Lead-Tin eutectic alloy, the sintering of Lead particles occurs during Superplastic deformation. They also found

evidence for grain boundary sliding. They studied the variation of texture with strain for a range of values of  $m$ . The texture of both Lead and Tin-rich phases has been measured in strip specimens produced by rolling the cast material at room temperature. It was shown that for  $m = 0.3$  to  $0.7$  the texture in Lead was completely removed after 200% strain, but the texture in Tin is weakened and changed upto the maximum strain investigated (500%). For the Lead-rich phase the angle between the rolling direction and the tensile axis influences the rate of change of texture, but not the final result. However, for the Tin-rich phase both the rate of change of texture and the details of the final texture depend on the angle between the tensile axis and rolling direction. Quantitative interpretation of the data was not possible as these texture measurements were confined to the central  $70^\circ$  of the stereogram. However, they pointed out that the general importance of grain boundary sliding, implied by many of the metallographic studies, is consistent with the texture measurements. They found that amount of sliding on Lead/Lead, Lead/Tin and Tin/Tin boundaries was different.

### 1.3 Applications

The behaviour of the Superplastic material is very similar to that of polymer materials and a number of workers<sup>81</sup> have emphasised the possibility of adapting established techniques for forming Polymers to the forming of Superplastic metals. The techniques include vacuum forming, drapes forming, bottle blowing etc.



There are two main advantages for forming of Superplastic materials:

- (i) Large strains can be obtained without the fear of localised necking, and
- (ii) The stresses under which Superplastic deformation occurs are low.

The main disadvantage in case of Superplastic materials is that low strain rates are required as compared with most conventional forming operations. However, the Lead-Tin eutectic is promising as this shows Superplasticity at relatively high value of strain rates.

Al-Naib and Duncan<sup>82</sup> have studied forming of Lead-Tin eutectic alloy. The large scale exploitation of Superplasticity by motor industry has been discussed by Hundy<sup>83</sup>. It was pointed out that the pattern of costs was very different from that encountered in conventional sheet-metal forming. However, Superplastic behaviour might be used industrially if complex welded assemblies could be replaced by a single Superplastically pressed component.

Theoretical analyses of metal forming operations for Superplastic materials have been reported<sup>19</sup>. In general, structural Superplasticity has received more attention for commercial exploitation than Environmental Superplasticity. However, one application of Environmental Superplasticity



has been reported by Johnson<sup>81</sup>. He describes the technique of die-less drawing.

The microstructural condition which gives Superplastic behaviour could also give rise to an improvement in a number of properties desirable in subsequent service. For example, it has been found that the creep-resistance is improved by Superplastic deformation during forming operation. However, there is a need for further explanation of the properties in materials after Superplastic deformation.

#### 1.4 Aim of Present Study

To begin with, this study was in continuation of Rawal's work<sup>84</sup> on commercial purity Lead-Tin eutectic. Three important findings of that work were :

- (i) Even large grain size (36) microns) material exhibited Superplastic behaviour.
- (ii) During Superplastic deformation recrystallisation was occurring which led to refinement of grain size, and
- (iii) With increasing amount of prior reduction, grain size was refined and better Superplastic behaviour resulted.

To gain a deeper insight and to minimise complications due to impurities in commercial purity materials, it was decided to work with high purity materials. The problem of As-cast eutectic having a fine structure but not exhibiting Superplasticity was also looked into. Starting with As-cast eutectic increasing amount of prior reduction was given. Superplastic behaviour of same grain sized material with

varying composition and processed differently has been reported by Cline and Alden<sup>15</sup>. Apart from the general observations about Superplastic behaviour we aimed at getting same grain size through different Thermomechanical processing keeping the composition same, and compare their mechanical behaviour to study whether Thermomechanical processing has some additional role besides the manipulation of grain size. Optical metallography was employed to study structural changes due to different Thermomechanical treatments and Superplastic deformation.

## CHAPTER 2

EXPERIMENTAL PROCEDURE2.1 Preparation

Eutectic alloy of Sn-38.1 wt.% Pb was cast in preheated, split-molds (Inner dia =  $\frac{1}{4}$ ", outer dia =  $1\frac{3}{8}$ ", length = 4.5") of mild steel. The melting was done, in air, in a graphite crucible. High purity (Appendix 1) materials were used. Solidified rods were immediately quenched in water. As-cast rods were swaged at, room temperature, in steps of 0.04" reduction in diameter. Care was taken to avoid excessive rise in temperature due to swaging. Following samples were chosen for study :

Table 2.1.

Identi- fication	Dia. after swaging	% Reduc- tion in Area	Annealed for 1 day	Annealed for 3 days	Annea- led for 7 days	Super- plasti- cally Deform- ed
A	0.34"	54%	A-1	A-3	A-7	SD-A
B	0.26"	73%	B-1	B-3	B-7	SD-B
C	0.18"	87%	C-1	C-3	C-7	SD-C
D	0.14"	92%	D-1	D-3	D-7	SD-D
E	0.10"	96%	E-1	E-3	E-7	-

As-cast and swaged rods were then machined to get specimens (A & B) of dimensions given in the Appendix 2. For others, rod-specimens were made such that gage length was greater than 4xDia., and their surface was cleaned using fine emery (3/0).

These specimens were all the time stored in deep freezer before testing in unannealed condition. All samples (A-E) were annealed at 120°C in air for various amounts of time (1 day, 3 days and 7 days). The identifications are given in above Table. Annealed samples were also stored in deep freezer prior to testing.

## 2.2 Testing

Instron (Floor model, TTC Standard, Low Speed Metric) was used for testing. Cross-head speeds could be changed incrementally from 0.004 cm/min. to 4 cm/min.  $n$  value was determined as follow. Cross-head speed was changed to a higher speed after there was about 3-4% elongation at a constant load. This results in a rise of load-level. This was repeated for all available cross-head speeds to cover a range of strain rates.  $n$  is given by

$$n = \frac{\log P_2/P_1}{\log V_2/V_1}, \quad P_2 > P_1 \quad \text{and} \quad V_2 > V_1$$

where,  $P$  = Load

$V$  = Cross-head speed.

This value of  $n$  was corresponding to lower strain rate, given by  $\dot{\epsilon} = \frac{V_1}{L}$ , where  $L$  equals instantaneous gage length. The values of  $n$  were calculated from load versus time plots.

Instantaneous gage length is computed by assuming the strain to be uniformly distributed along the entire gage length. This is a valid assumption.

Tests were conducted to find elongation at constant cross-head speed corresponding to that strain rate which gave

peak  $m$  for that sample. These tests were conducted for all samples (A-E). Tests were conducted on annealed samples also. Values of stress and strain rate refer to the true values. After giving about 3-4% steady state strain at all available cross-head speeds, this procedure was repeated to study behaviour in II cycle.

### 2.3 Metallography

The samples were mechanically polished using Liquid Paraffin to avoid scratches. Silk-cloth was used for final polishing on a Polishing wheel moving at low speed. A suspension of 0.005 micron Polishing compound was used for Polishing wheel. A washing-powder solution was used to avoid scratches due to Polishing wheel.

The polished samples were etched with a freshly prepared reagent suggested by Avery and Bookofen<sup>1,24</sup>. It consists of :

1 Part Nitric Acid.

1 Part Acetic Acid

and 8 Parts Glycerol.

After etching photo-micrographs were taken. The initial magnification was 500 and 800 and it was further magnified 2.2 times to get prints of B2 size. Kodak, low-speed, fine grain, 80 ASA, 35 mm film was used. Pictures were taken soon after the test to avoid the complication of grain growth at room temperature.

## CHAPTER 3

### RESULTS & DISCUSSION

#### 3.1 Initial Microstructural Observations

The grain size was measured from photomicrographs of the polished and etched samples by Linear Intercept method. Random lines at various orientations were drawn on the photomicrograph. The number of intersections counted was about one hundred or more. This gave an accuracy of  $\pm 0.1$  micron in the measurements (Appendix 3). A modification of Linear intercept method (Appendix 2) to account for two phase nature of the Pb-Sn eutectic, could not be applied because of no clear-cut distinction between grains of both phases and/or the structure being intermixed type, i.e., it was not clear where one particle of second phase ends and the other begins or the grains of second phase were more or less continuous. The grain size in our case refers to metallographic mean free path and it was assumed that grain size equals interparticle distance. The grain sizes of various samples are listed in Table 3.1.

The matrix is Tin-rich phase and occupies 71% volume. The dark phase or second phase is Lead-rich phase.

As-cast Pb-Sn eutectic alloy has lamellar structure at many points (Interlamellar spacing equals 1 micron, Fig.2,3). At other points lamellae have degenerated into

### Table 3.1

[illegible]



nonuniformly distributed and irregular shaped particles of various sizes (Fig.4,5). The grain size is 1.10 microns.

With 54% prior reduction (hot working) the lamellar structure is completely lost and everywhere the long lamellae are degenerated into fine particles. The clustering of particles occurs now only at relatively fewer places. The grain size is 1 micron (Fig.6,7).

With increase in prior reduction to 73%, the grain size remains same at 1.00 micron but the clustering of second phase particles occurs at still fewer places (Fig.8).

With further increase in prior reduction to 87%, the grain size becomes 0.98 microns. The second phase is quite uniformly distributed (Fig.9).

After 87%, as prior reduction is increased to 92%, coarsening of second phase occurs. The grain size is 1.90 microns. The structure is intermixed, i.e., the grains of second phase are more or less continuous or it is not clear where one grain ends, and the other begins (Fig.10).

With further increase in prior reduction to 96% an equiaxed structure is obtained in which the two phases are separate grains and interphase boundaries are relatively smooth. The grain size is 1.70 microns. In general, the particles of second phase are longer in one dimension than the other. This might suggest the retention of basic lamellar

structure though the length of the lamellae is reduced very much and parallel alignment of the lamellae is lost which was observed in the As-cast eutectic. In the case of 96% prior reduction, some rounding of second phase particles occurs, i.e., the structure is tending to be equiaxed.

The effect of annealing at 120°C for varying amounts, on samples having different prior reductions was studied. Comparing the structure of 54% prior reduction sample after annealing for 1, 3 and 7 days, it was found that grain size increased from 1.00 micron in the unannealed state to 1.35, 1.90 and 2.30 microns respectively. Before annealing the structure was very fine (Fig.6,7) and the two phase were separate grains and interphase boundaries were relatively smooth, though some clustering was also present. By annealing the structure becomes intermixed type (Fig.12). The second phase particles are longer in length than in width though they are not straight. The intermixed character is lost by annealing for 7 days when an equiaxed structure is obtained in which two phases are separate grains and interphase boundaries are relatively smooth.

For 73% prior reduction, the grain size increases from 1.00 micron in the unannealed state to 1.36, 1.90 and 2.20 microns after annealing for 1, 3 and 7 days respectively. The interphase boundaries are sharp throughout, i.e. after annealing for 1, 3 and 7 days. After annealing for 7 days the grain boundaries of the matrix were also revealed at some places.

For 87% prior reduction, the grain size increased from 0.98 microns in the unannealed state to 1.69, 1.90 and 2.40 microns after annealing for 1, 3 and 7 days respectively. After annealing for 1 day, the interphase boundaries remain sharp and grain boundaries of parent matrix are revealed. After annealing for 3 days the structure remains same except for coarsening. The grain boundaries of the parent matrix are still visible. After annealing for 7 days the structure becomes intermixed type.

For 92% prior reduction, annealing for 1 day produced a grain size of 1.70 microns as compared with 1.90 microns in the unannealed state. The structure is intermixed type in the unannealed state. After annealing for 1 day the interphase boundaries become clear. After annealing for 3 days the structure shows two phases as separate grains and interphase boundaries are relatively smooth. The grain size is 1.79 microns. After annealing for 7 days the structure becomes intermixed type and the grain size is 2.10 microns.

For 96% prior reduction, the unannealed structure has two phases as separate grains and grain size is 1.70 microns. It becomes 2.00 microns and structure becomes intermixed type after annealing for 1 day. After annealing for 3 days, the grain size becomes 2.25 microns and again the two phases occur as separate grains, the interphase boundaries being clear and smooth. After annealing for 7 days the grain size increases further to 2.80 microns and the structure becomes intermixed type.

From the observations above it became clear that:

(i) Upto 87% prior reduction there is no change in grain size. After 92% prior reduction coarsening occurred.

(ii) By annealing, coarsening of grain size occurred in general. The structure was not stable as it alternates between intermixed type, where the grains of second phase are more or less continuous, and clear-cut type where the two phases occur as separate grains and interphase boundaries are clear and smooth.

(iii) For small prior reductions the particles of second phase are longer in length than in width. They are not straight but are curved in a zig-zag fashion. With increasing amount of prior reduction the structure tends to become equiaxed.

(iv) Samples B-7 and E-1 give same grain size of 2.00 microns, though they have widely varying mechanical and thermal history. B-7 has 73% prior reduction and has been annealed for 7 days and E-1 has 96% prior reduction and has been annealed for 1 day.

### 3.2 Mechanical Data

Following information was obtained from tension tests on Instron:

As-cast material (Fig.31) shows a low value of  $m$  ( $\approx 0.15$ ) at all strain rates, for room temperature tests. The elongation was small and the fractured surface clearly showed a blow hole. This observation was made in all the three As-cast samples tested. However, the number of blow holes was only very small. The microstructure recorded (Figs. 2 - 5) did not show any blow-holes.

With increase in prior reduction (Fig.31)  $m$  values increase. Upto 73% prior reduction no peak in the  $m$  vs. strain rate curves was observed upto the minimum strain rate studied ( $3.2 \times 10^{-3} \text{ min}^{-1}$ ). From 87% prior reduction onwards a peak is observed at the intermediate strain rate. In all cases the peak is rather broad, indicating occurrence of high  $m$  values in a broader band of strain rates. The maximum value of  $m = 0.45$  was observed in two cases - one for 73% prior reduction at  $3.20 \times 10^{-3} \text{ min}^{-1}$  and the other for 96% prior reduction at  $4.6 \times 10^{-2} \text{ min}^{-1}$ .

With strain-rate cycling it was found (Fig.32) that  $m$  values are higher in second cycle even upto 87% prior reduction.

Increasing the test temperature improves the  $m$  values considerably (Fig.33). The peak  $m$  was 0.48 at  $6 \times 10^{-2} \text{ min}^{-1}$  for a sample with 54% prior reduction. With increasing prior reduction, the improvement in  $m$  values due to test temperature is better. The peak is shifted to higher strain rates. Thus,

the effect of increasing prior reduction and increasing test temperature is similar — both shift the peak to the higher strain rates.

With annealing the  $m$  values go down and peak is shifted to lower strain rates. When prior reduction is more, the  $m$  values for annealed samples approach, at low strain rates, the values that are higher than those for unannealed samples at those strain rates (Figs. 34 - 38).

The  $\log \sigma - \log \dot{\epsilon}$  curves are S-shaped in some cases (the corresponding  $m$  vs. strain rate curves of these showed a peak) (Fig.40). With increasing prior reduction the true stress decreases. There is a large decrease in stress values from 73% prior reduction to 87% prior reduction though the grain size remains nearly same. No correlation between grain size and true stress could be obtained.

With strain-rate-cycling (Fig.41) it was found that increasing prior reduction reduces the difference in stress values for the first and second cycle. For 87% and 92% prior reduction, the true stress values did not change with strain-rate-cycling. This indicates that with increasing prior reduction the structure remains stable during Superplastic elongation. In our case the minimum prior reduction to attain a relatively stable structure was 87%.

With increasing test temperature (Fig.42) stress values are lowered but the nature of  $\log \sigma$  vs.  $\log \dot{\epsilon}$  curve remains unchanged.



With increasing annealing time the true stress values increase (Figs. 43 - 46) but the nature of  $\log \sigma$  vs.  $\log \dot{\epsilon}$  curve remains unchanged. This increase is observed upto annealing for 3 days. Further annealing either does not change the stress (Figs. 46,45) values or decreases the stress level (Fig.43). This indicates that the structure becomes stable after annealing for 3 days. No correlation between grain size and true stress was obtained.

In a constant cross-head speed test (Fig.49), it was found that in a sample with 54% prior reduction the true stress value dropped with % elongation at room temperature and this drop was reduced to a very small value at 120°C test temperature. In a sample with 92% prior reduction (Fig.50), the true stress remained more or less constant with increasing elongation. With annealing for various amounts the true stress falls with increasing elongation. This was observed in other samples also which had different amounts of prior reduction. This effect may be due to the grain growth during deformation and/or from the contribution of decreasing strain rate with increasing strain (strain rate becomes half for every 100% elongation) to flow stress. Ideally, the test should be done at constant strain rate in order to separate out the contributions of structural changes and strain rate<sup>87</sup>.

A few cross-plots were also made. Comparing the  $m$  vs.  $\dot{\epsilon}$  strain rate plots (Fig.39) of same grain-sized material processed differently, a large difference in  $m$  values was found. It



Therefore,  $\int f dV(\mu^{(x)}) \leq ||x|| \int f d\lambda + \epsilon$ . Since  $\epsilon > 0$  is arbitrary, we get  $\int f dV(\mu^{(x)}) \leq ||x|| \int f d\lambda$ . This shows that  $V(\mu^{(x)}) \leq ||x|| \lambda$ . Hence for any  $E \in \Sigma$ ,  $|\mu^{(x)}(E)| \leq V(\mu^{(x)})(E) \leq ||x|| \lambda(E)$ . Therefore,  $||\mu_L(E)|| \leq \lambda(E)$ . Since this is true for any  $E \in \Sigma$ , we have  $V(\mu_L) \leq \lambda$ . Thus  $\mu_L$  is of bounded variation and is regular. Hence  $\mu_L \in M(S, X^*)$ , and also  $||\mu_L||_V \leq ||\lambda||_V = ||L||$ .

From the definitions, it is clear that  $x \circ \mu_L = \mu^{(x)}$  for any  $x \in X$ . So if we take  $F \in C_0(S, X)$  of the form  $F = \sum_{i=1}^n f_i x_i$ , with each  $x_i \in X$  and each  $f_i \in C_0(S)$ , then from Proposition 2.5 and 2.6, it easily follows that  $\int F d\mu_L = L(F)$ . Since the functions of this form are dense in  $C_0(S, X)$ , we have  $L(F) = \int F d\mu_L$  for any  $F \in C_0(S, X)$ . It also follows that  $|L(F)| = |\int F d\mu_L| \leq ||F||_\infty ||\mu_L||_V$ , and hence  $||L|| \leq ||\mu_L||_V$ . Since we have already proved  $||\mu_L||_V \leq ||L||$ , we have  $||\mu_L|| = ||L||$ . Moreover, it is easy to see that the correspondence  $L \mapsto \mu_L$  is linear and our proof is complete.

Note: If  $G$  is a locally compact abelian group, then the correspondence of  $C_0(G, X)^*$  and  $M(G, X^*)$  will be taken in the following way for convenience,

$$\langle \mu, F \rangle = \int_G F(-x) d\mu(x).$$

**2.9 Product Measures:** Let  $(X, Y, Z)$  be a bilinear system of Banach spaces. Let  $S$  and  $T$  be locally compact Hausdorff spaces and let  $S \times T$  be their cartesian product.

It shows both intermixed type structure and the other type in which interphase boundaries are clear. For 73% prior reduction sample, the grain size increases from 1.00 micron to 2.20 microns after 200% Superplastic elongation (Fig.28). The interphase boundaries are smoother. For 87% prior reduction, the grain size increases from 0.98 microns to 2.20 microns after 300% Superplastic elongation (Fig.29). The interphase boundaries remain smooth. For 92% prior reduction sample, the grain size increases from 1.90 microns to 2.30 microns after 100% Superplastic elongation (Fig.30). The interphase boundaries remain smooth. Thus, in general, coarsening of structure occurs by Superplastic elongation but interphase boundaries remain smooth and structure remains relatively equiaxed. Coarsening also occurred by annealing but by annealing the interphase boundaries are zig-zag and the second phase particles are not equiaxed.

### 3.4 Discussion

As-cast structure is not Superplastic because the structure is predominantly lamellar. This is in conformity with the findings of earlier workers.

With increasing prior reduction, recrystallisation and/or grain growth change the initial lamellar structure to a relatively more equiaxed structure. The sudden change in grain size is possibly due to heating by mechanical work put in by swaging. Increasing prior reduction leads to a relatively more stable structure which changes only very

little by Superplastic elongation. When prior reduction is less the structure is relatively unstable during Superplastic elongation.

The processing history determines the shape of the second phase particle. Prior reduction produces a coarsened but equiaxed structure. Annealing also produces coarsening but the second phase particles are elongated and have zig-zag shape. Earlier workers have found evidence for a large contribution of grain boundary sliding in Superplastic elongation in Pb-Sn eutectic. If this is so, our observation that annealing is detrimental to Superplastic behaviour and prior reduction is beneficial though both lead to a coarsening of structure, can be explained on the basis that prior reduction produces equiaxed structure and annealing produces elongated grains with zig-zag boundaries which are a hinderance for grain boundary sliding. Comparing the behaviour of same grain-sized material processed differently, a difference in behaviour was observed because of different contributions of mechanical and thermal processing.

In this study, the variation in grain size obtained by different mechanical and thermal processing was only a few microns. Even the coarsest structure obtained was fine from the point of view of criteria for observing Superplasticity.

In Pb-Sn eutectic, Avery and Backofen<sup>1</sup> found that true stress is proportional to  $L^2$ . Later on Martin and Backofen<sup>24</sup>

found that true stress is proportional to  $L^a$ , where  $a$  equals 0.5 - 0.9. From our study it appears that the uncertainty in grain size dependence of flow stress arises because of variation in processing history. We did not find an exact correlation between grain size and flow stress. With Superplastic elongation the grain size increased while true stress decreased. This is probably due to smooth nature of interphase boundaries. The irregular boundaries lead to a higher value of true stress. Another observation substantiates this. The initial true stress,  $I$ , decreased with increasing prior reduction. Also, with increasing prior reduction a relatively equiaxed structure with smooth interphase boundaries is obtained. This emphasises the importance of the nature of interphase boundaries in determining the Superplastic behaviour of Pb-Sn eutectic. Strain-enhanced coarsening has been studied in eutectoid steels, in which the lamellar structure can be rapidly changed by hot working to the typical structure of spheroids of cementite in a ferrite matrix normally obtained by long-term annealing<sup>88,89</sup>. The stress vs. strain curves in this case show a drop with continued strain. It was suggested that the spheroidisation process can be enhanced by cold work followed by annealing, but hot work is more effective.

- - -

## CHAPTER 4

### CONCLUSIONS

Following conclusions can be drawn from the present study.

1. As-cast Pb-Sn eutectic is not Superplastic.
2. The Superplastic behaviour is enhanced by prior reduction by swaging which leads to a relatively equiaxed structure.
3. Annealing is detrimental to Superplastic behaviour in Pb-Sn eutectic as it leads to elongated grains with zig-zag interphase boundaries.
4. The shape of the second phase particle and the nature of interphase boundary are important factors in determining Superplastic behaviour. Even the same grain sized materials behave differently if the shape of the second phase particles is different. A relatively equiaxed structure shows better Superplastic properties than an assymmetric structure with zig-zag interphase boundary.

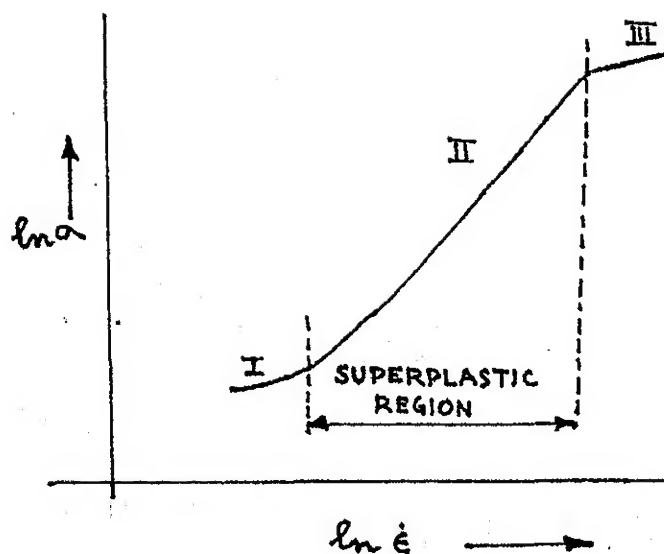
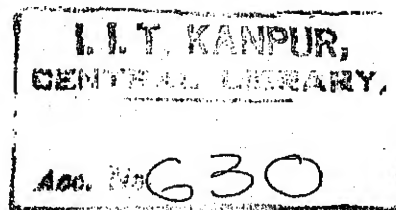


FIG.1 SCHEMATIC REPRESENTATION OF  
STRAIN RATE DEPENDENCE OF  
TRUE FLOW STRESS FOR SUPERPLASTIC  
MATERIALS



LEAD-TIN EUTECTIC

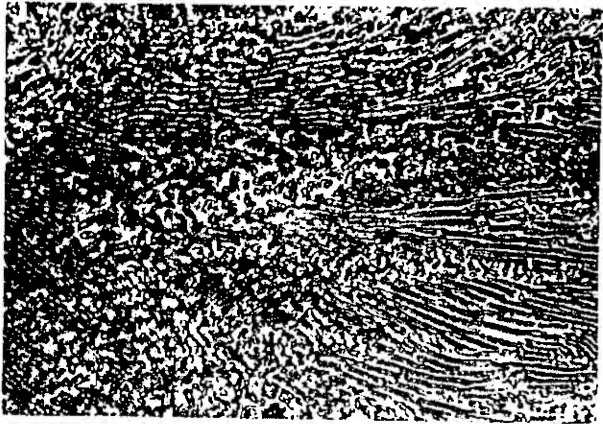


Fig.2 As-Cast, Lamellar  
Structure X 1110.

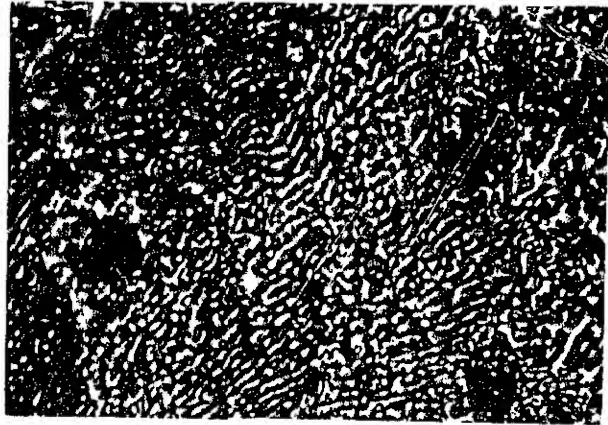


Fig.3 As-Cast, Lamellar  
Structure X 1760.

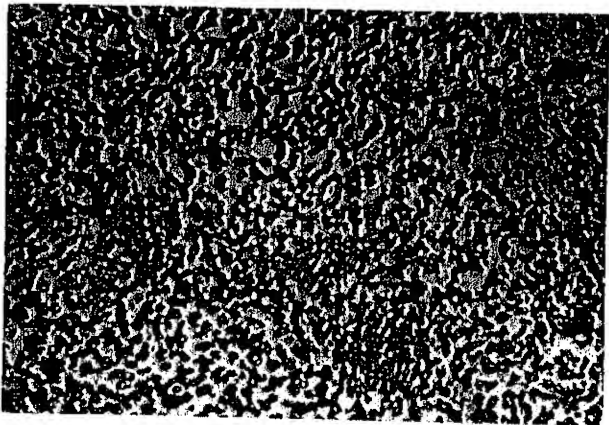


Fig.4 As-Cast, Nonlamellar  
Region, X 1110,  
 $L = 1.10 \mu$

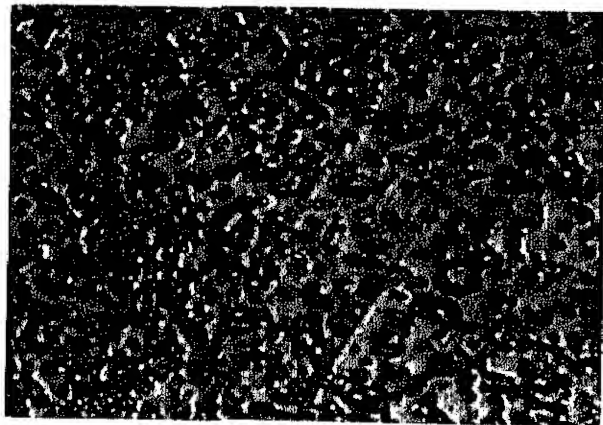


Fig.5 As-Cast, Nonlamellar  
Region, X 1760,  
 $L = 1.10 \mu$



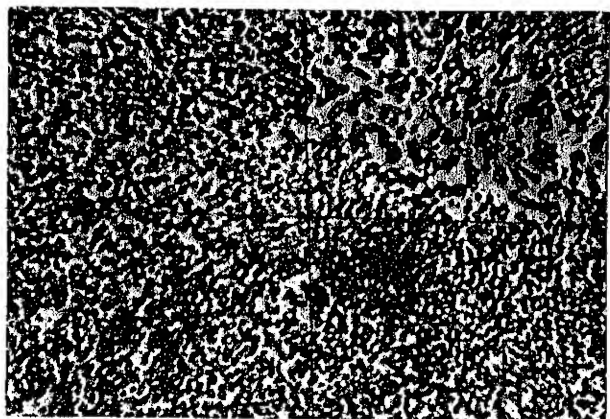


Fig.6 A:Swaged to 0.34",  
% Reduction in  
Cross-Section = 54%,  
X 1110, L = 1.00 $\mu$

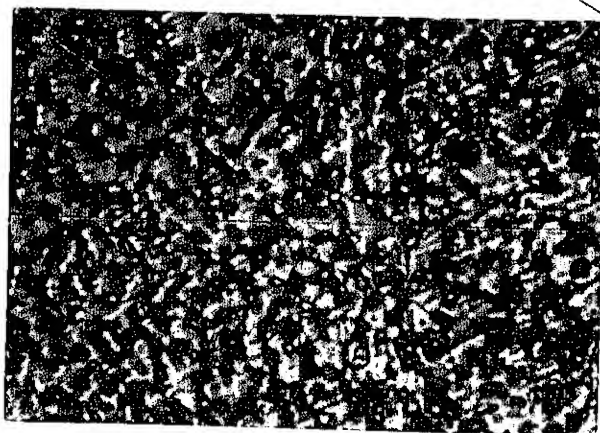


Fig.7A: Swaged to 0.34",  
% Reduction in  
Cross-Section = 54%,  
X 1760, L = 1.00 $\mu$

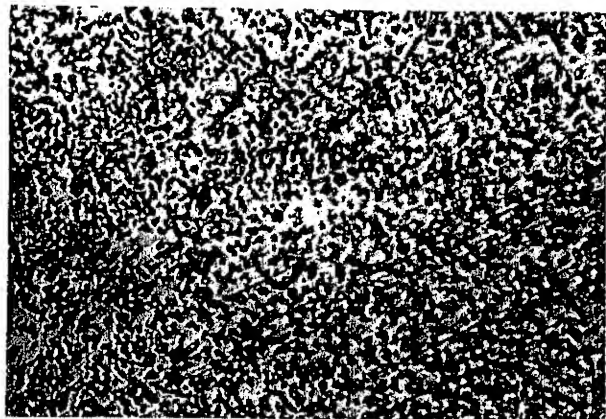


Fig.8 B:Swaged to 0.26",  
% Reduction in  
Cross-Section = 73%,  
X 1110, L = 1.00 $\mu$

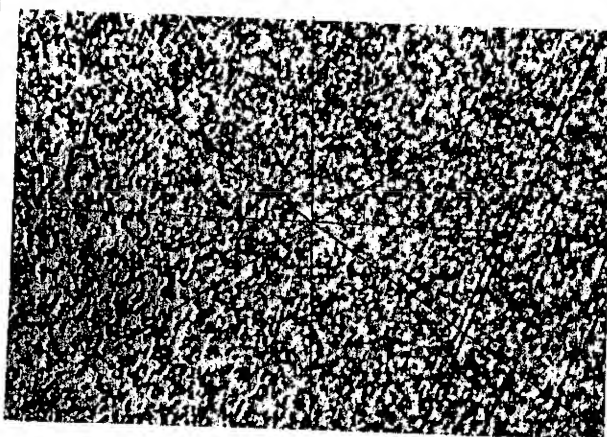


Fig.9 C:Swaged to 0.18",  
% Reduction in  
Cross-Section = 87%,  
X 1110, L = 0.98 $\mu$

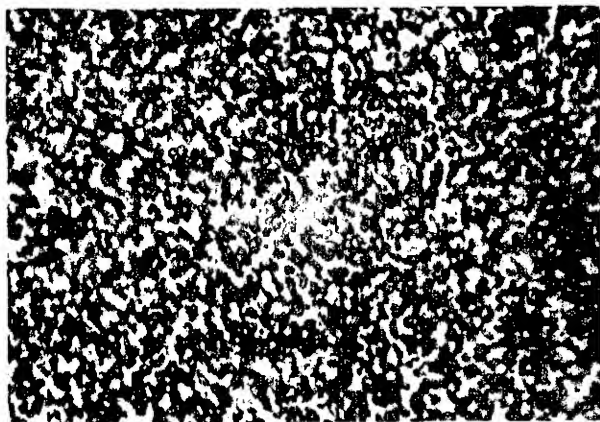


Fig.10 D:Swaged to 0.14",  
% Reduction in  
Cross-Section = 92%,  
X 1110,  $L = 1.90\mu$

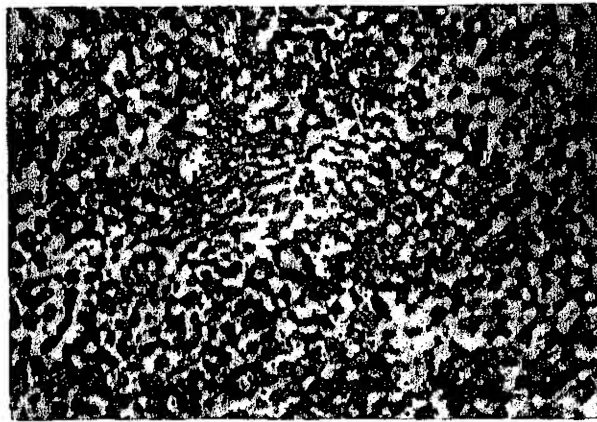


Fig.11 E:Swaged to 0.10",  
% Reduction in  
Cross-Section=96%,  
X 1110,  $L = 1.70\mu$

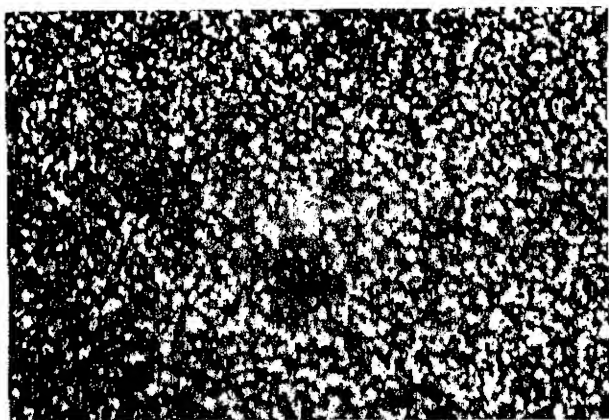


Fig.12 A-1:Annealed at 120°C  
for 1 day, X 1110,  
 $L = 1.35\mu$

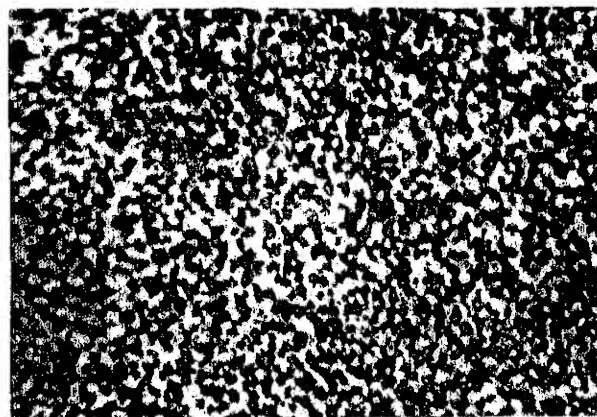


Fig.13 B-1:Annealed at 120°C  
for 1 day (24 hours),  
X 1110,  $L = 1.36\mu$

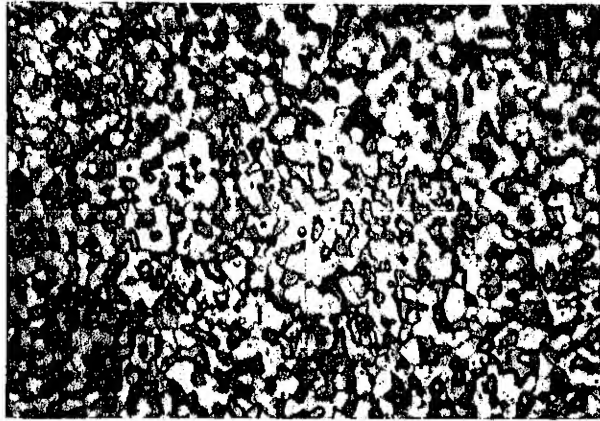


Fig.14 C-1: Annealed at 120°C  
for 1 day, X 1110,  
 $L = 1.69\mu$

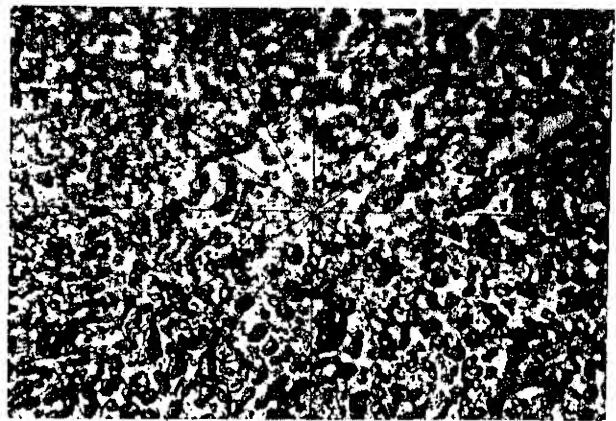


Fig.15 D-1: Annealed at 120°C  
for 1 day, X 1110,  
 $L = 1.70\mu$

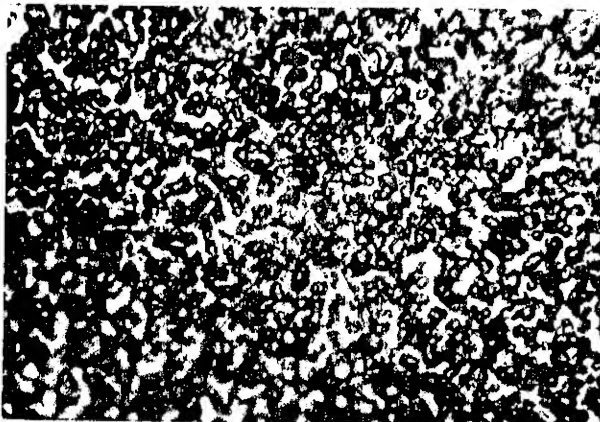


Fig.16 E-1: Annealed at 120°C  
for 1 day, X 1110,  
 $L = 2.00\mu$

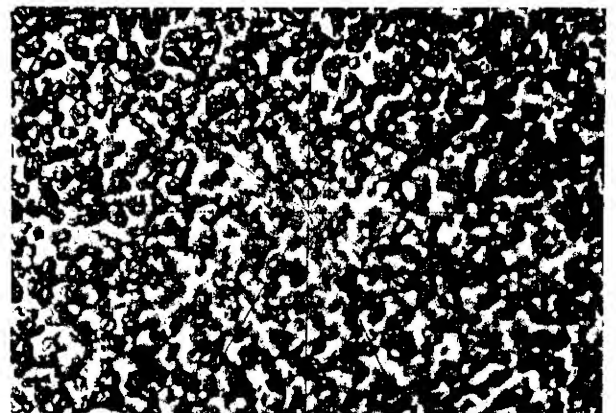


Fig.17 A-3: Annealed at 120°C  
for 3 days (72 hours),  
X 1110,  $L = 1.90\mu$

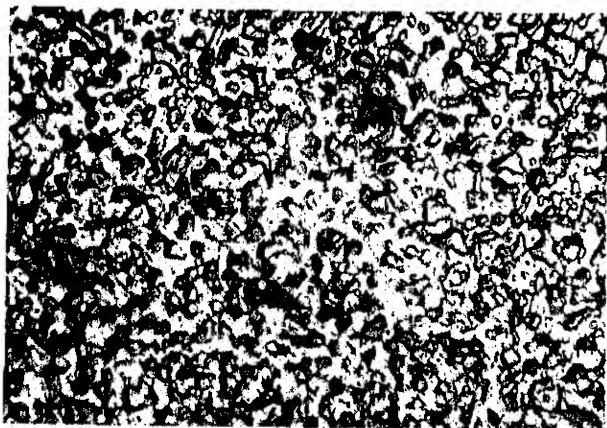


Fig.18 B-3: Annealed at 120°C  
for 3 days, X 1110, "  
 $L = 1.90\mu$

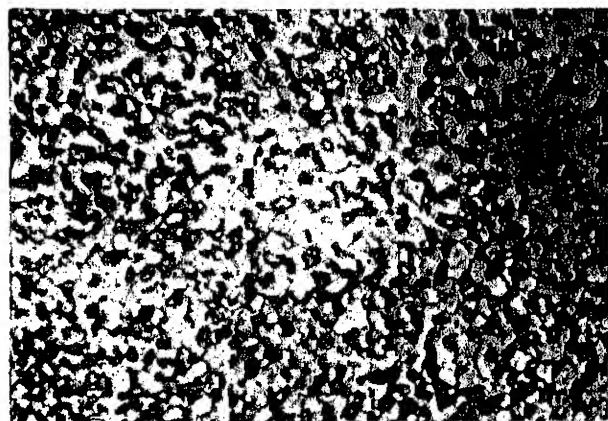


Fig.19 C-3: Annealed at 120°C  
for 3 days, X 1110, "  
 $L = 1.90\mu$

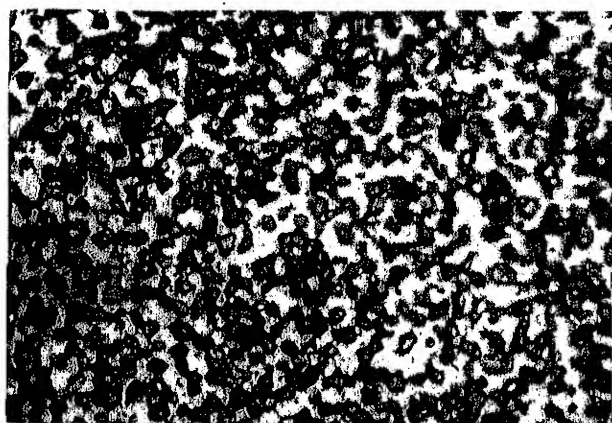


Fig.20 D-3: Annealed at 120°C  
for 3 days, X 1110, "  
 $L = 1.79\mu$

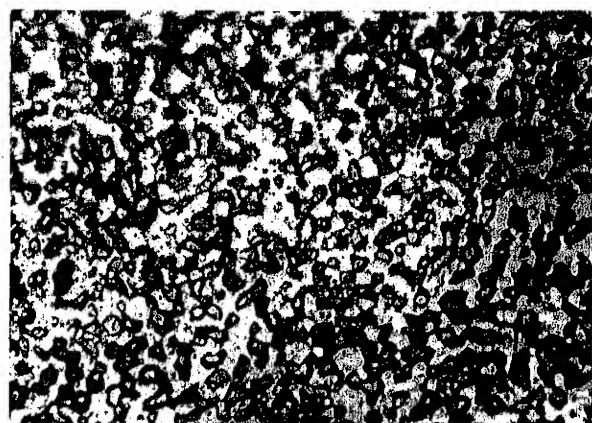


Fig.21 E-3: Annealed at 120°C  
for 3 days, X 1110, "  
 $L = 2.26\mu$



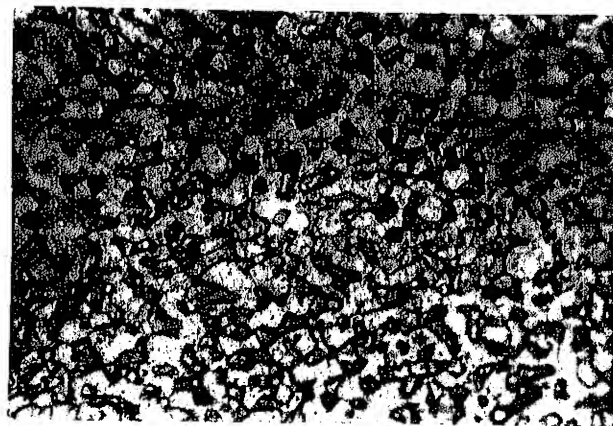


Fig.22 A-7: Annealed at 120°C  
for 7 days, X 1110,  
 $L = 2.30\mu$

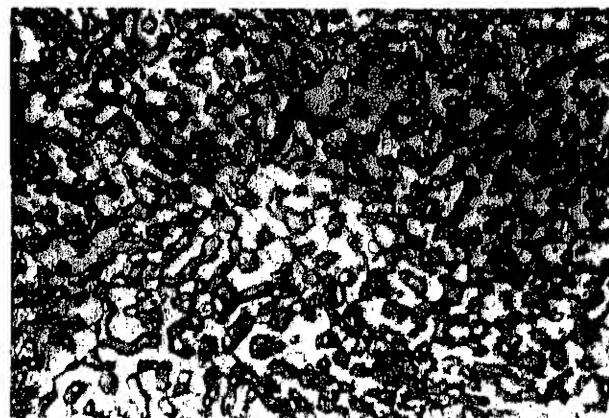


Fig.23 B-7: Annealed at 120°C  
for 7 days, X 1110,  
 $L = 2.00\mu$

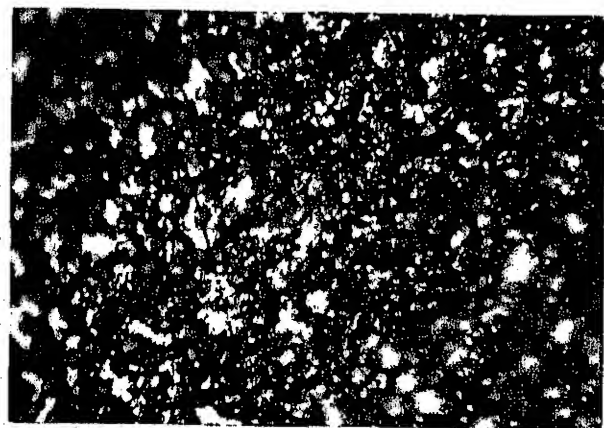


Fig.24 C-7: Annealed at 120°C  
for 7 days, X 1110,  
 $L = 2.40\mu$

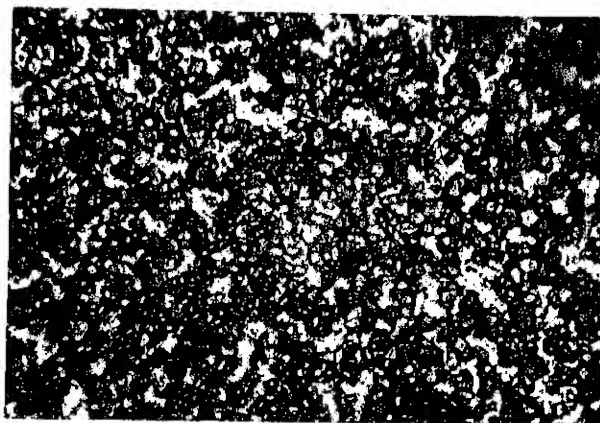


Fig.25 D-7: Annealed at 120°C  
for 7 days, X 1110,  
 $L = 2.10\mu$

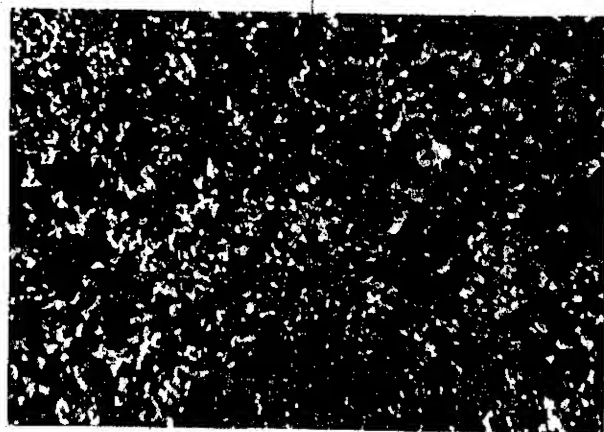


Fig.26 E-7: Annealed at 120°C  
for 7 days, X 1110,  
L = 2.80 $\mu$

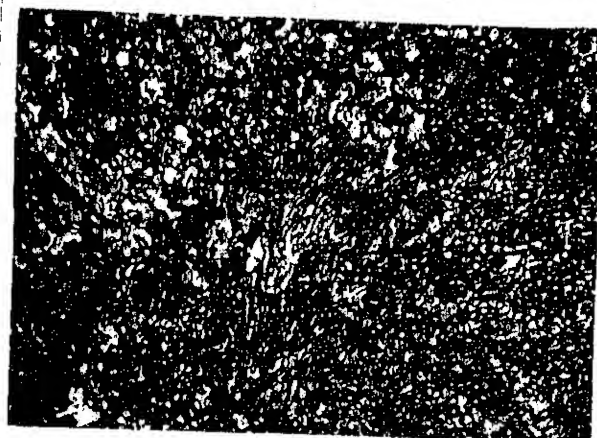


Fig.27 SD-A: 150% Elongation,  
X 1110, L = 2.00 $\mu$



Fig.28 SD-B: 200% Elongation,  
X 1110, L = 2.20 $\mu$

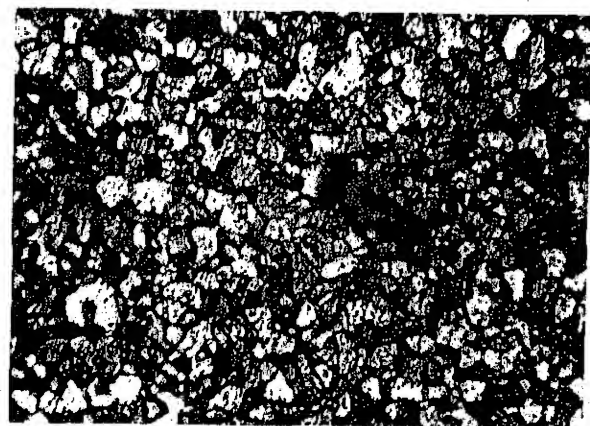


Fig.29 SD-C: 300% Elongation,  
X 1110, L = 2.20 $\mu$

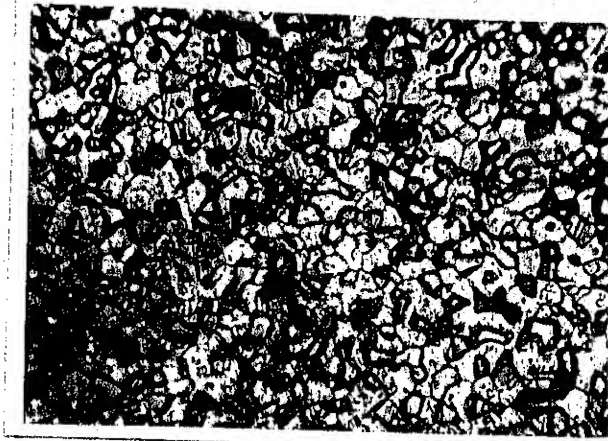


Fig.30 SD-D: 100% Elongation,  
X 1110, L = 2.30 $\mu$



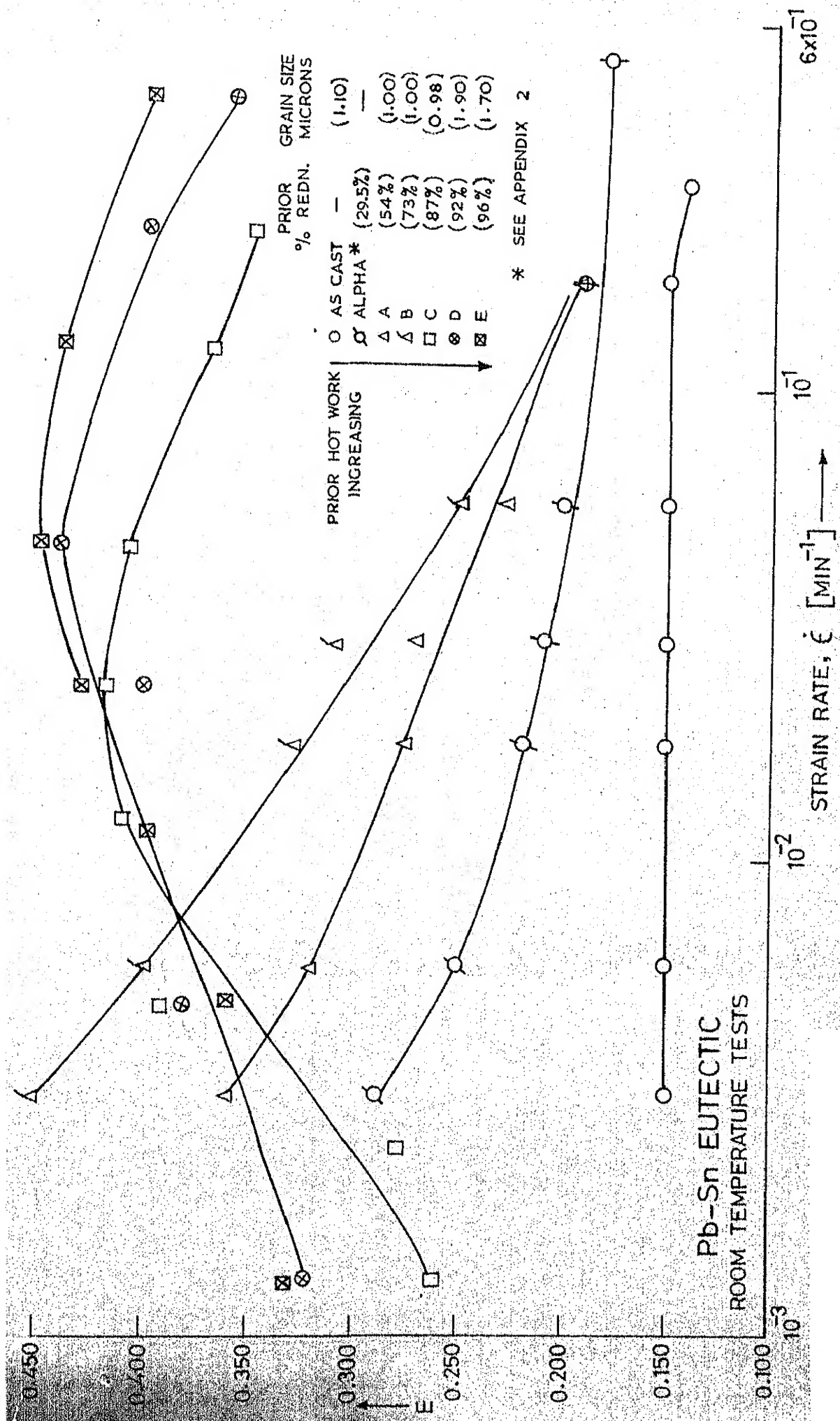


FIG. 31 STRAIN RATE DEPENDENCE OF  $m$  AT ROOM TEMP.

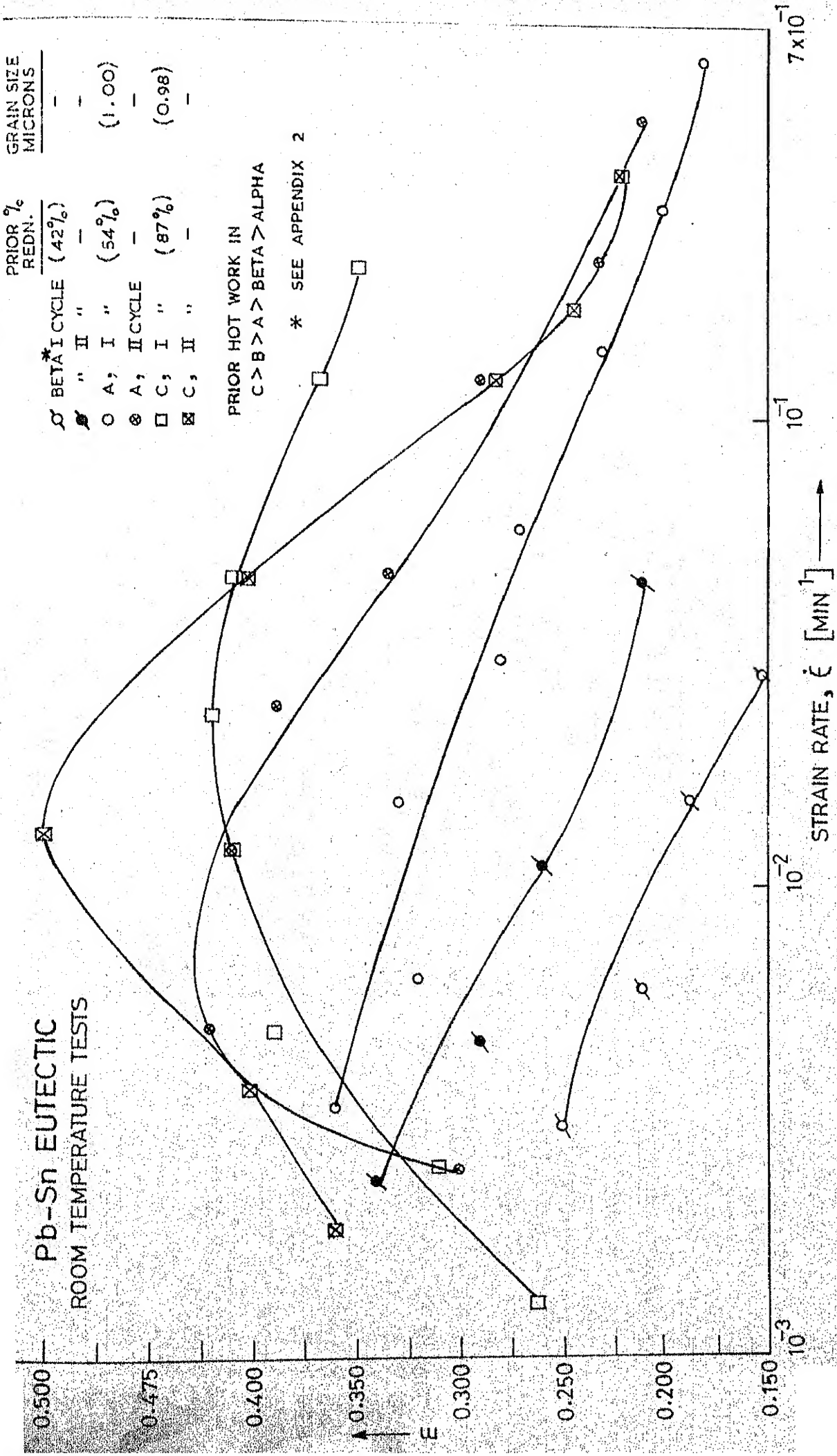


FIG.32 EFFECT OF STRAIN RATE CYCLING ON  $m$  vs. STRAIN RATE BEHAVIOUR

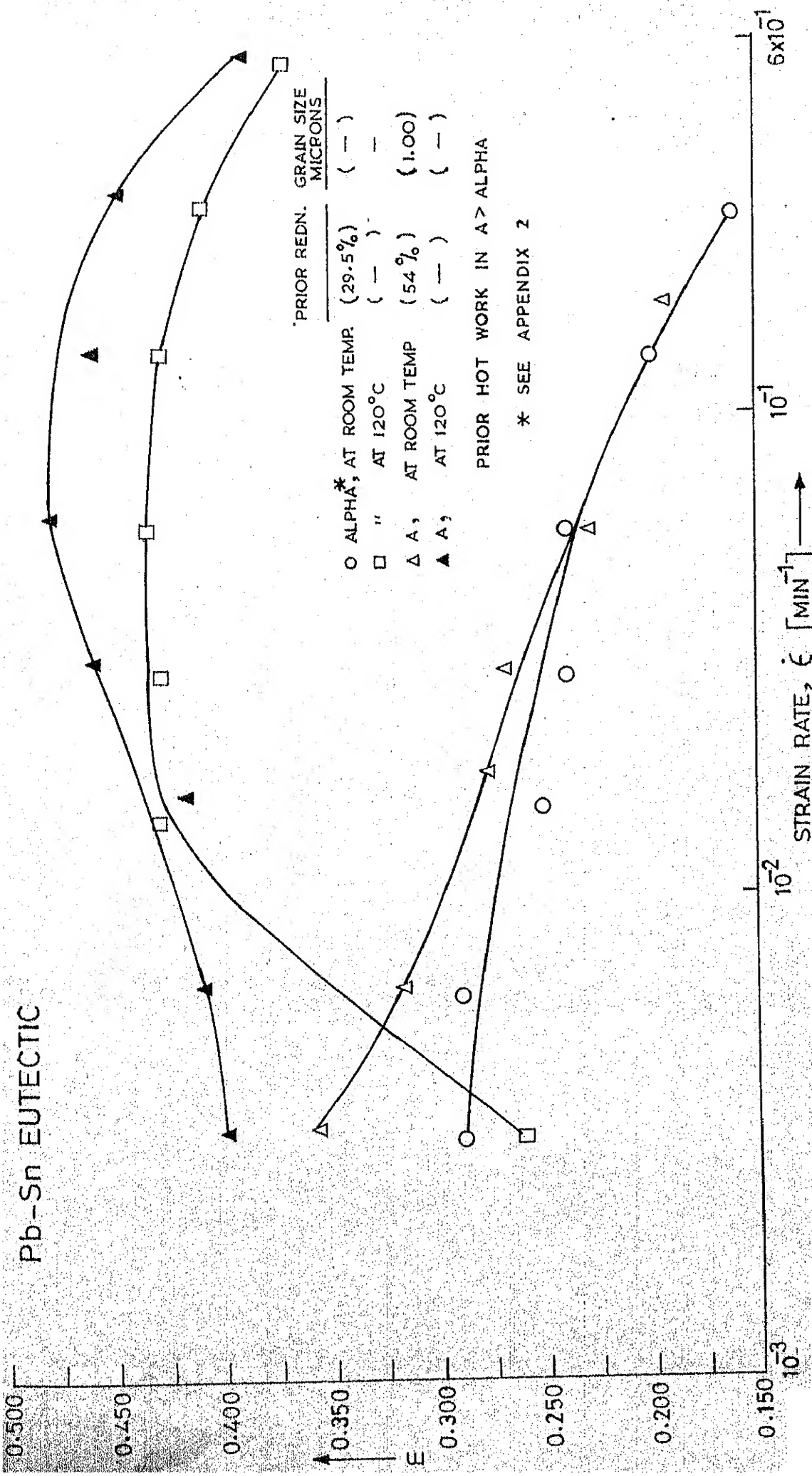


FIG.33 EFFECT OF TEST TEMPERATURE ON m vs. STRAIN RATE BEHAVIOUR

Pb-Sn EUTECTIC  
54 % PRIOR REDUCED

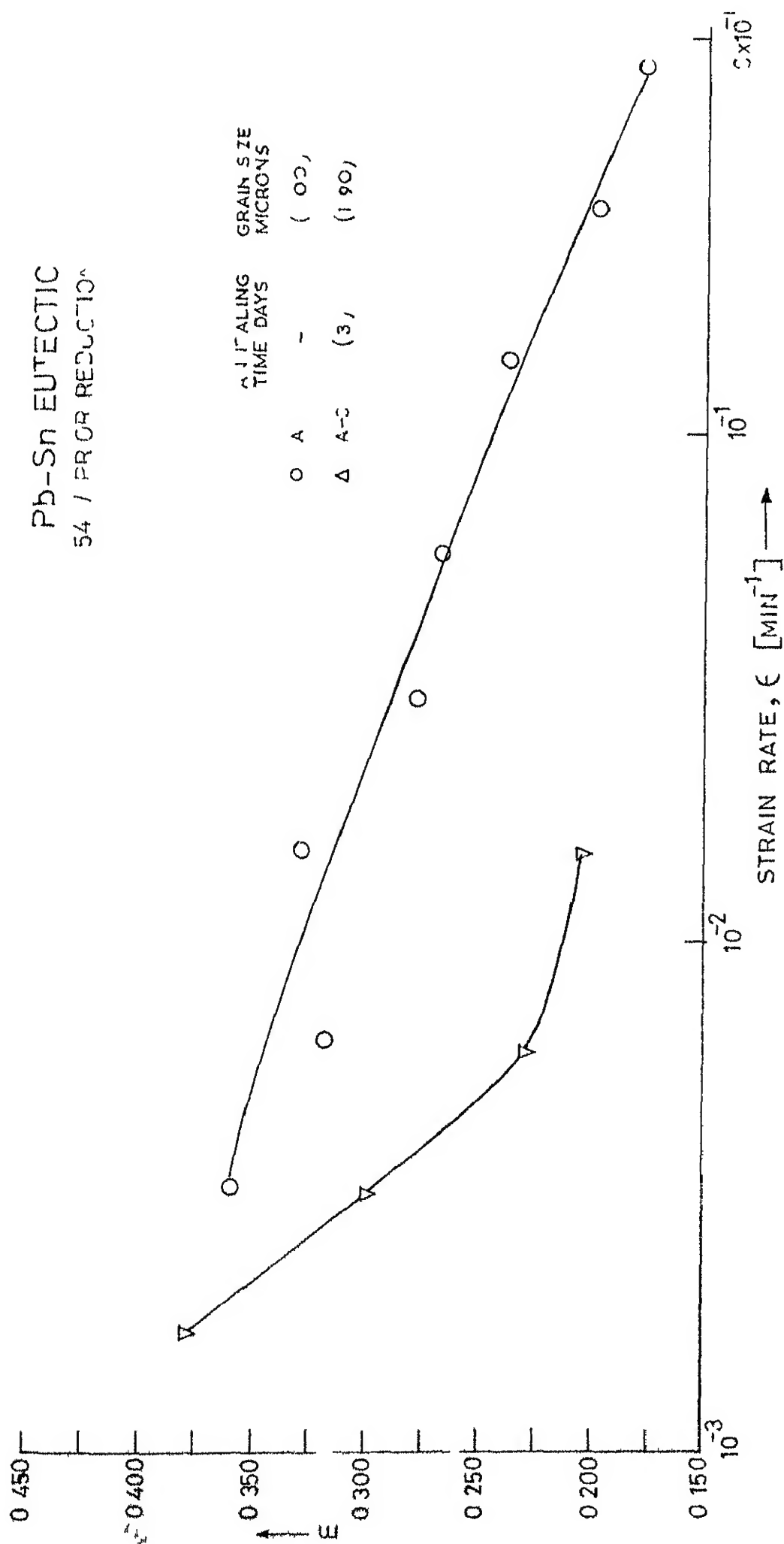


FIG 34 EFFECT OF ANNEALING ON  $m$  vs  $\epsilon$  BEHAVIOUR (54 % PRIOR REDN )

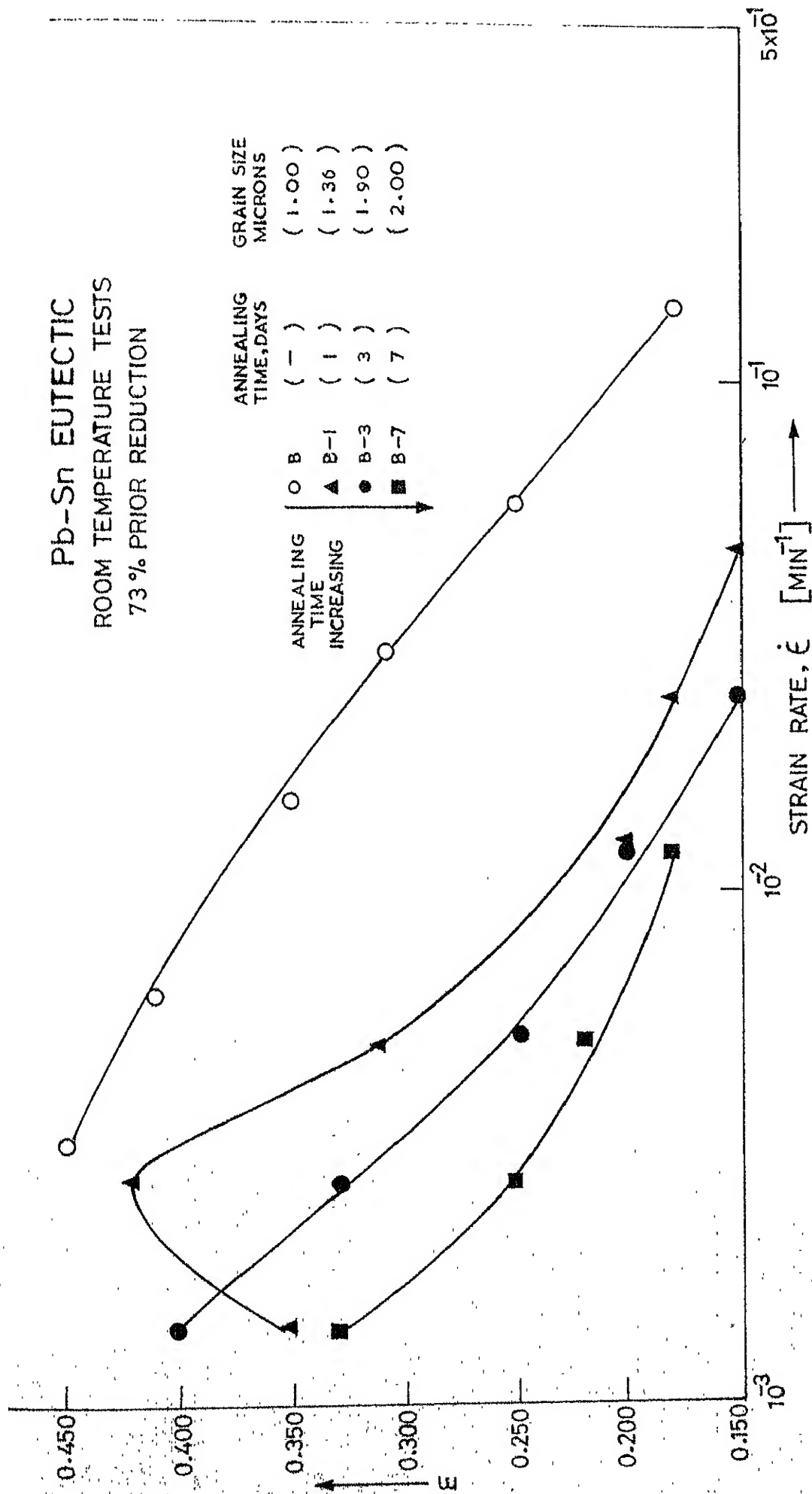


FIG.35 EFFECT OF ANNEALING ON  $\epsilon$  vs. STRAIN RATE BEHAVIOUR (73% PRIOR REDN.)

Pb-Sn EUTECTIC  
ROOM TEMPERATURE TESTS  
87% PRIOR REDUCTION

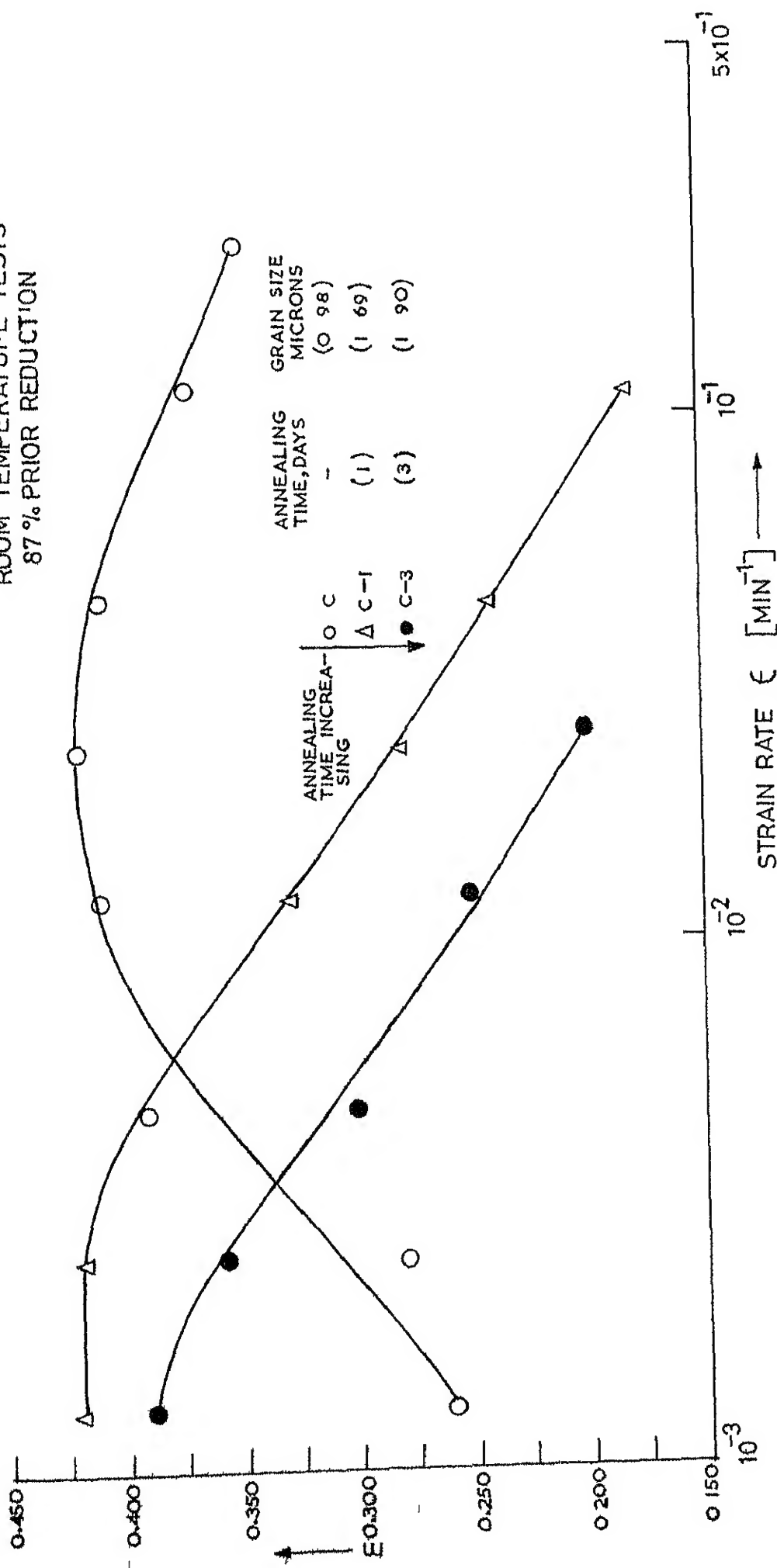


FIG 36 EFFECT OF ANNEALING ON  $m$  vs STRAIN RATE BEHAVIOUR (87% PRIOR REDN)

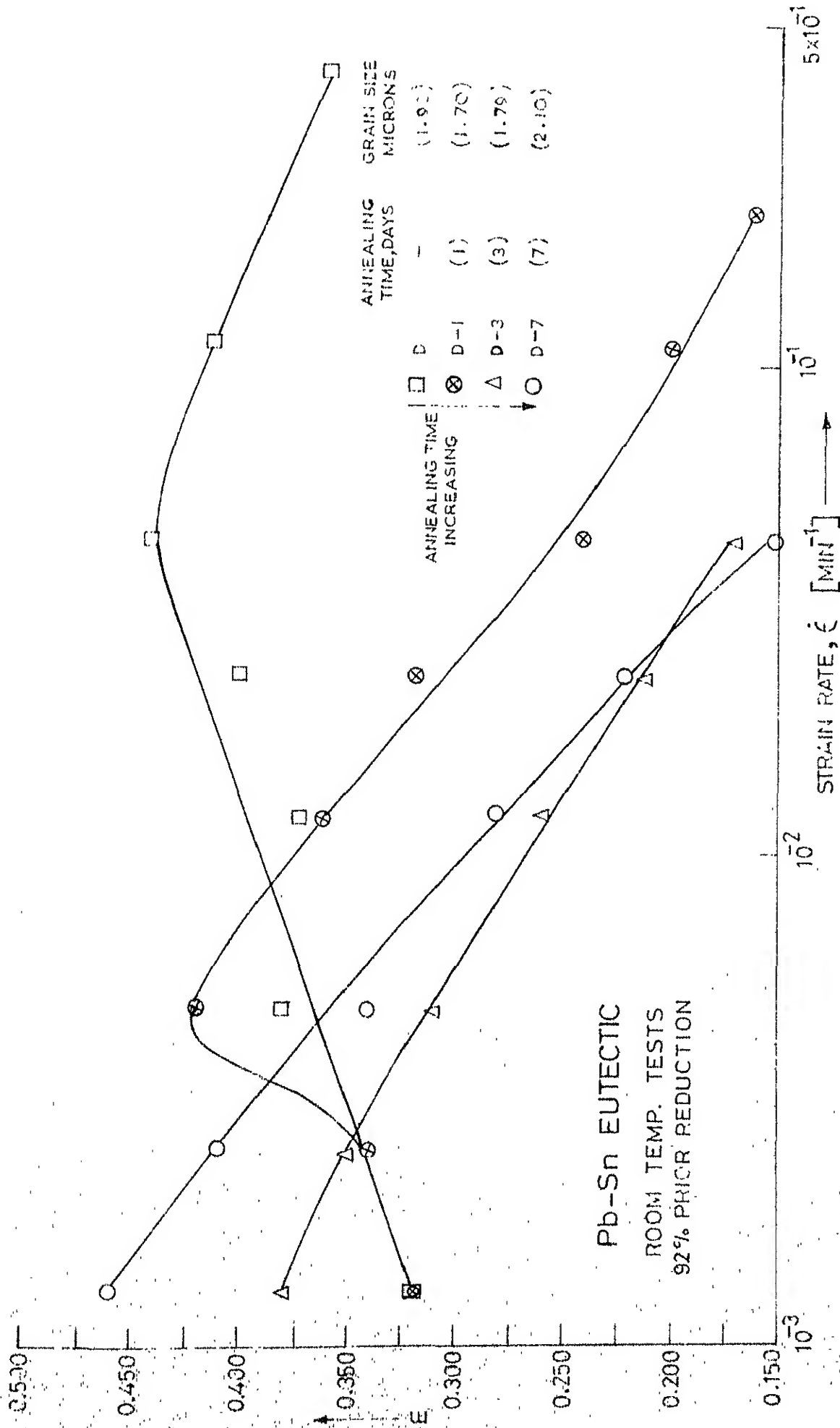


FIG.37 EFFECT OF ANNEALING ON  $m$  vs  $\dot{\epsilon}$  BEHAVIOUR (92% PRIOR REDUCTION)



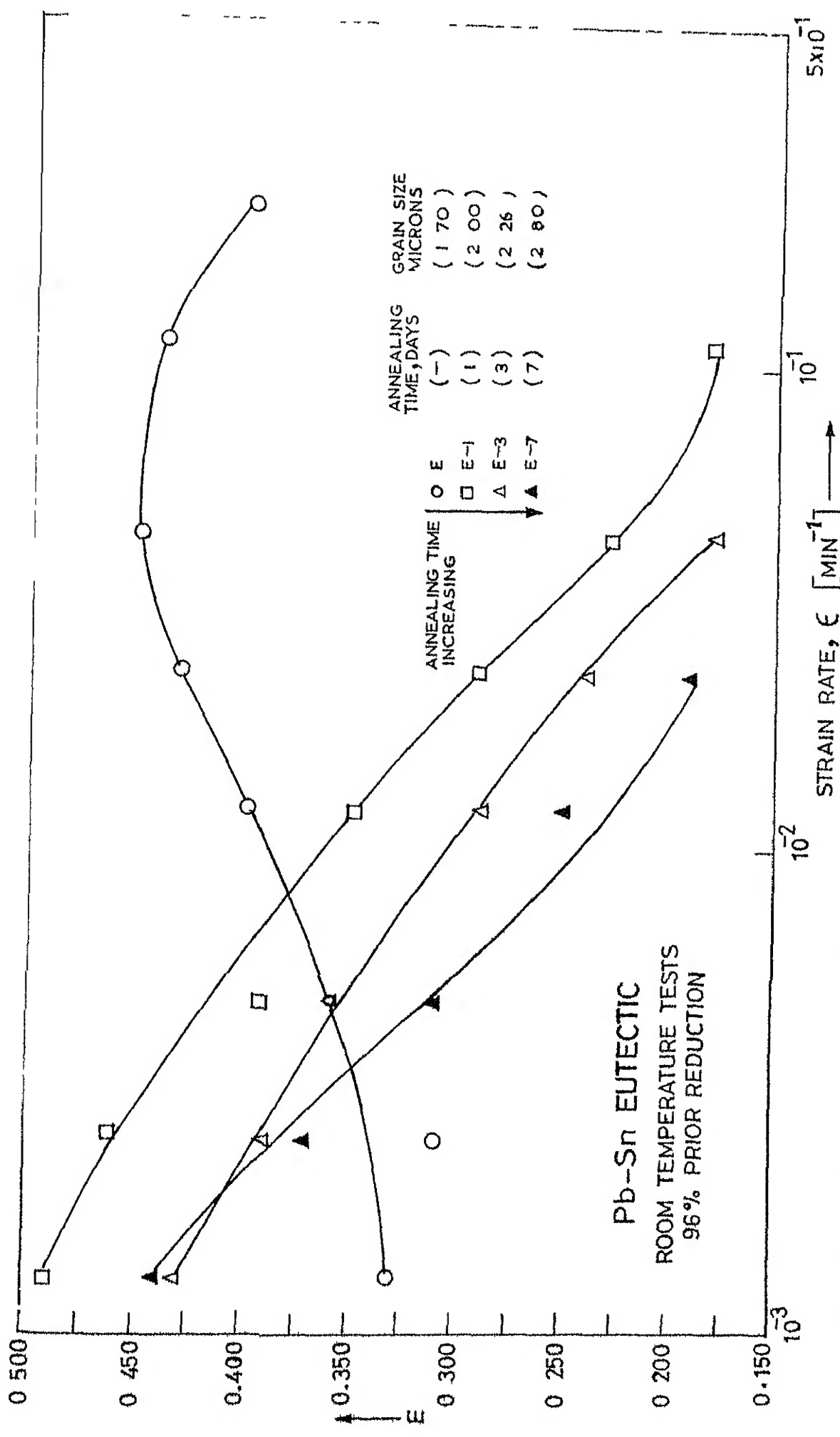


FIG.38 EFFECT OF ANNEALING ON  $m$  vs STRAIN RATE BEHAVIOUR (96 % PRIOR REDN )

# Pb-Sn EUTECTIC ROOM TEMPERATURE TESTS

	PRIOR REDUCTION	ANNEALING TIME DAYS	GRAIN SIZE MICRONS
□	E-1 (96%)	(1)	(2 00)
○	B-7 (73%)	(7)	(2 00)

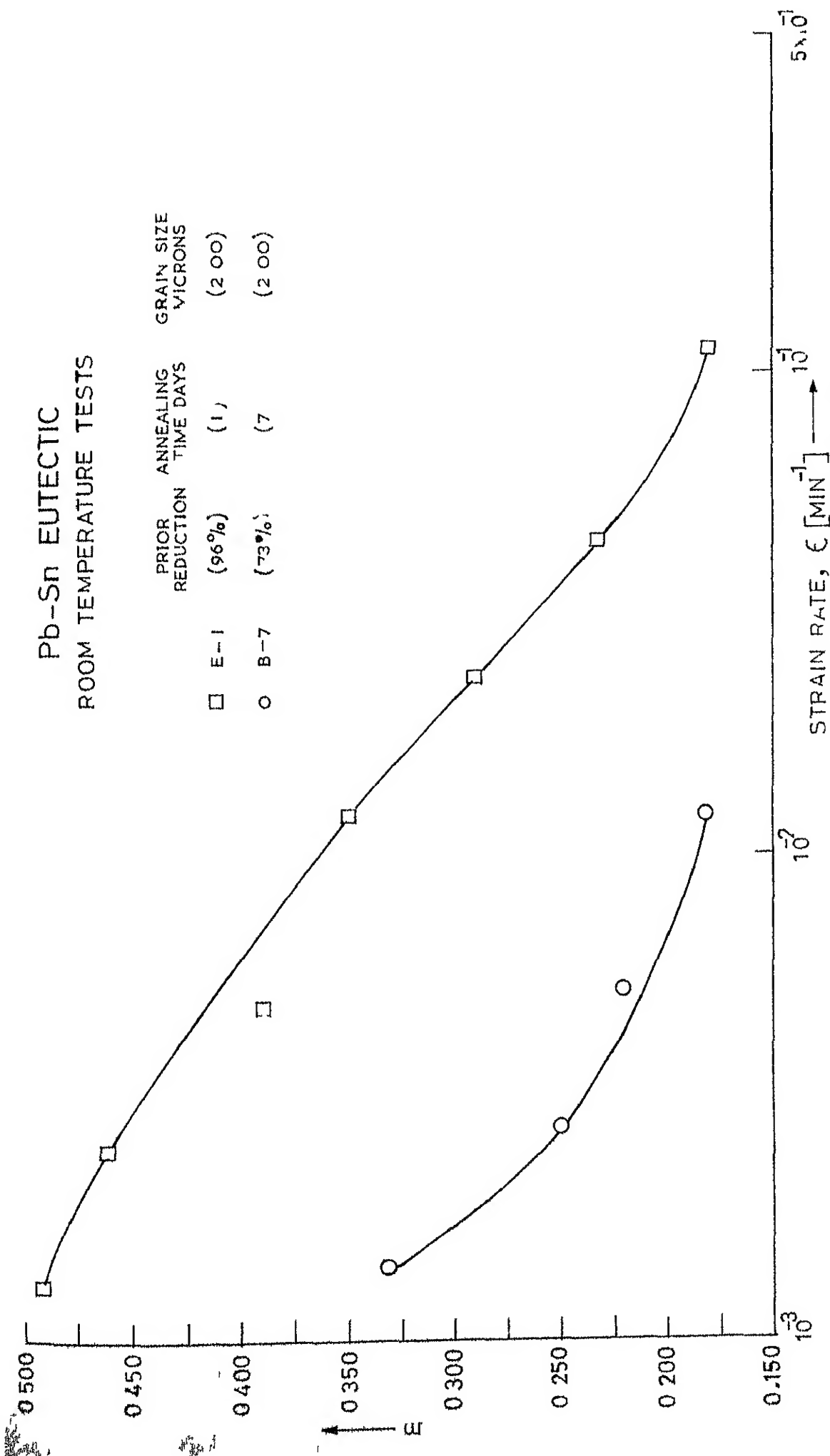


FIG 39  $\sigma$  vs.  $\dot{\epsilon}$  BEHAVIOUR OF SAME GRAIN SEIZED MATERIAL PROCESSED DIFFERENTLY

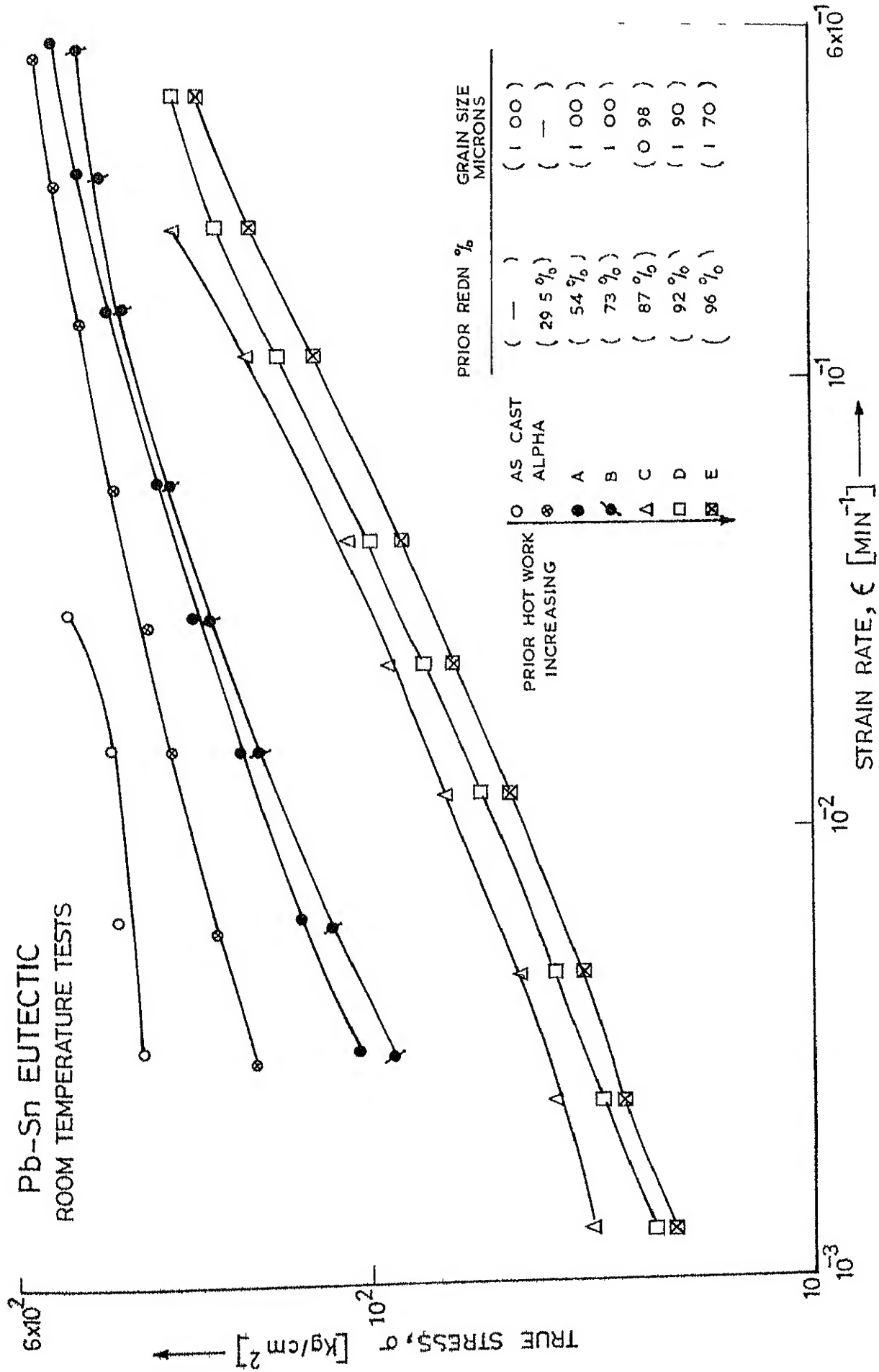


FIG 40 STRAIN RATE DEPENDENCE OF TRUE STRESS AT ROOM TEMP

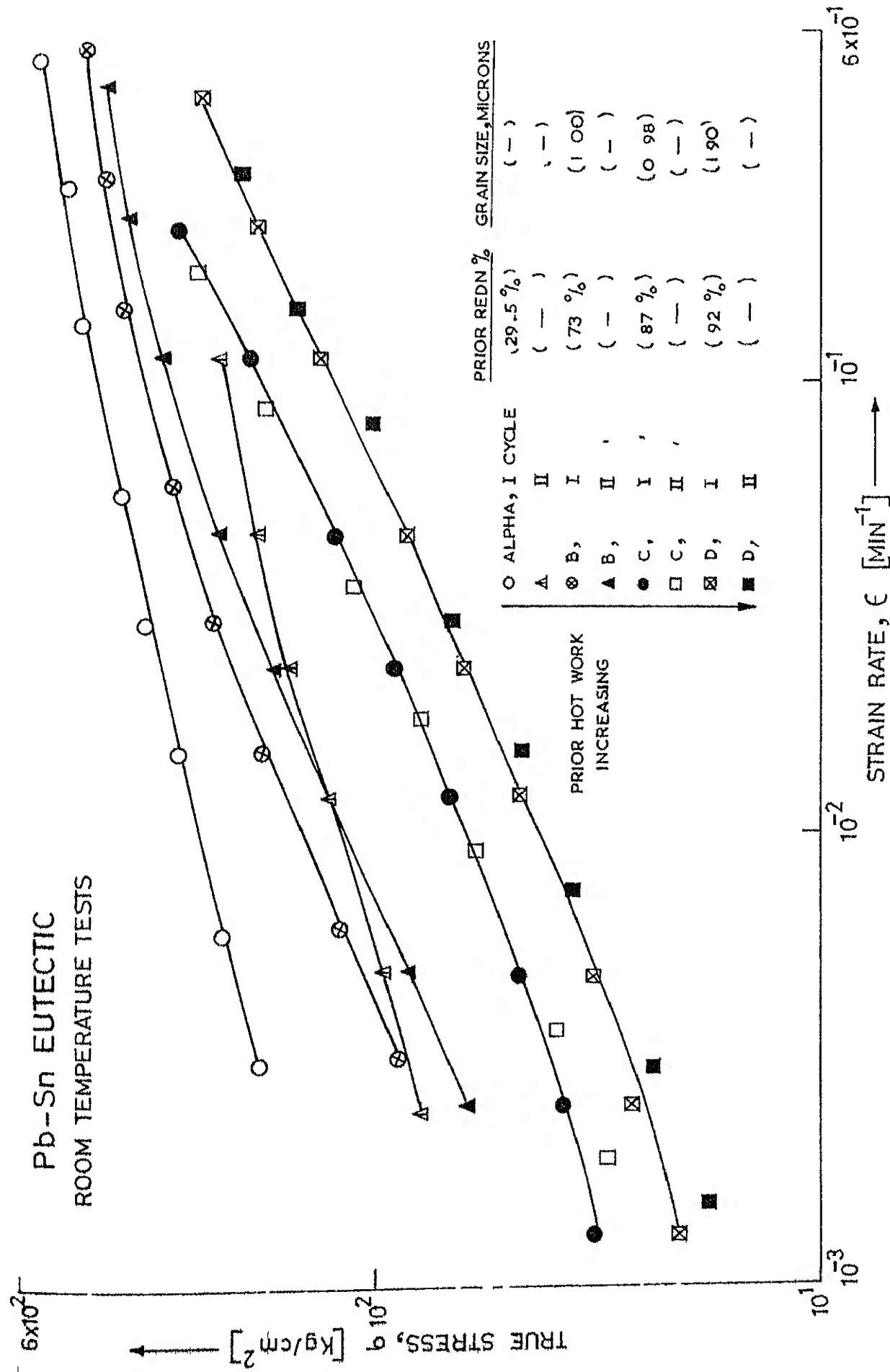


FIG 41 EFFECT OF STRAIN RATE CYCLING ON TRUE STRESS vs STRAIN RATE BEHAVIOUR

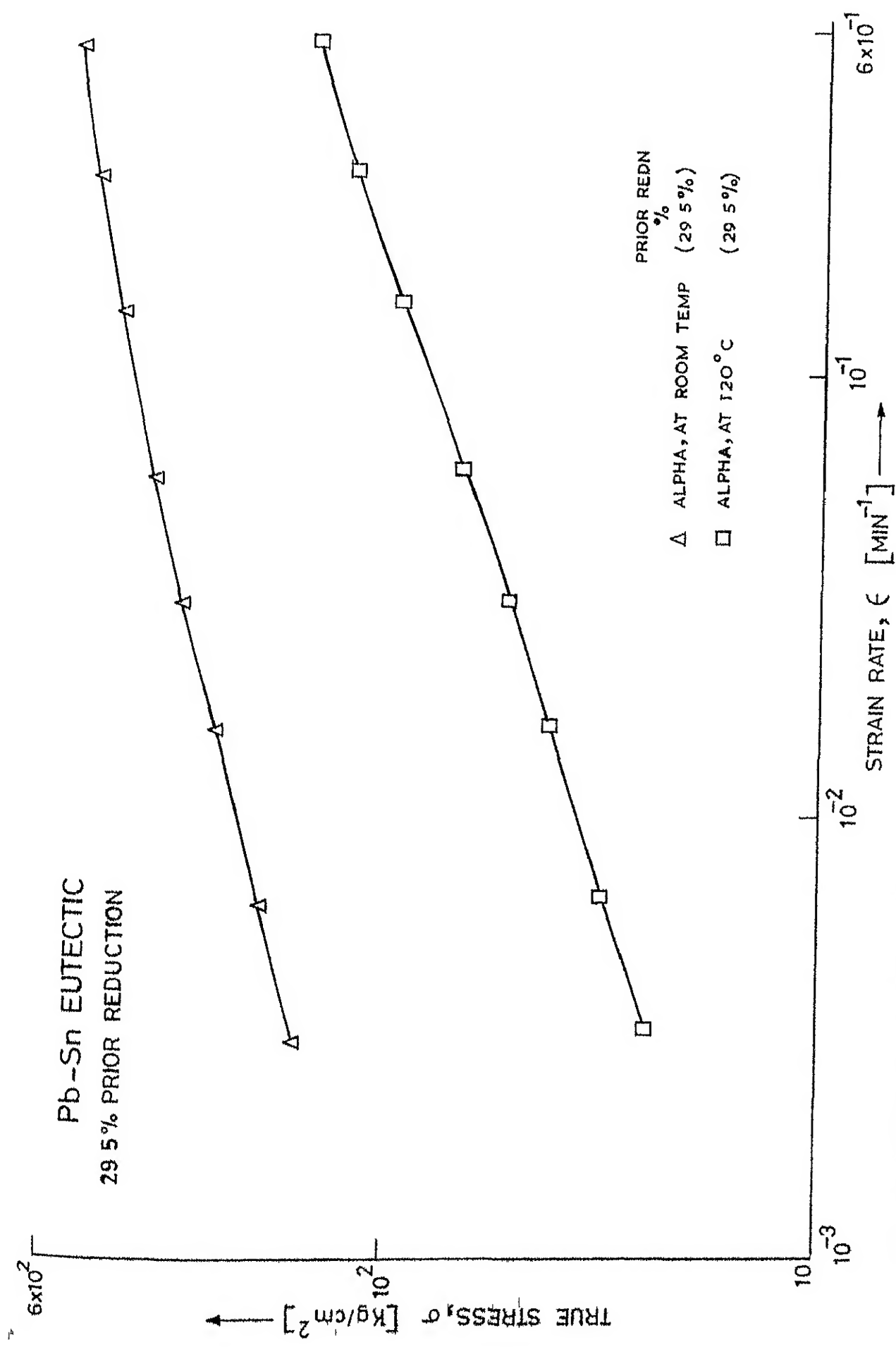


FIG.42 EFFECT OF TEST TEMPERATURE ON  $\sigma$  vs  $\epsilon$  BEHAVIOUR (29.5% PRIOR REDN)

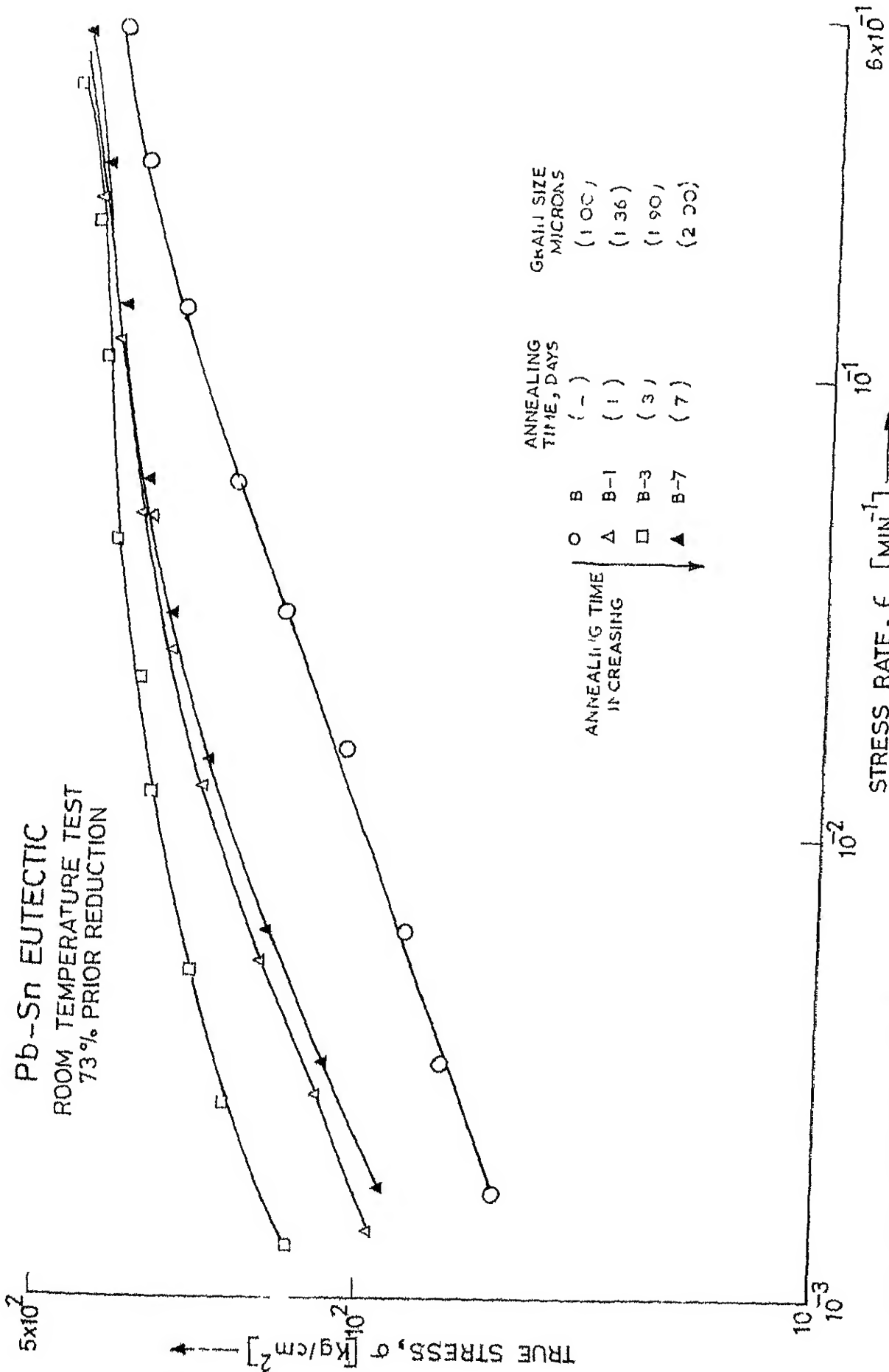
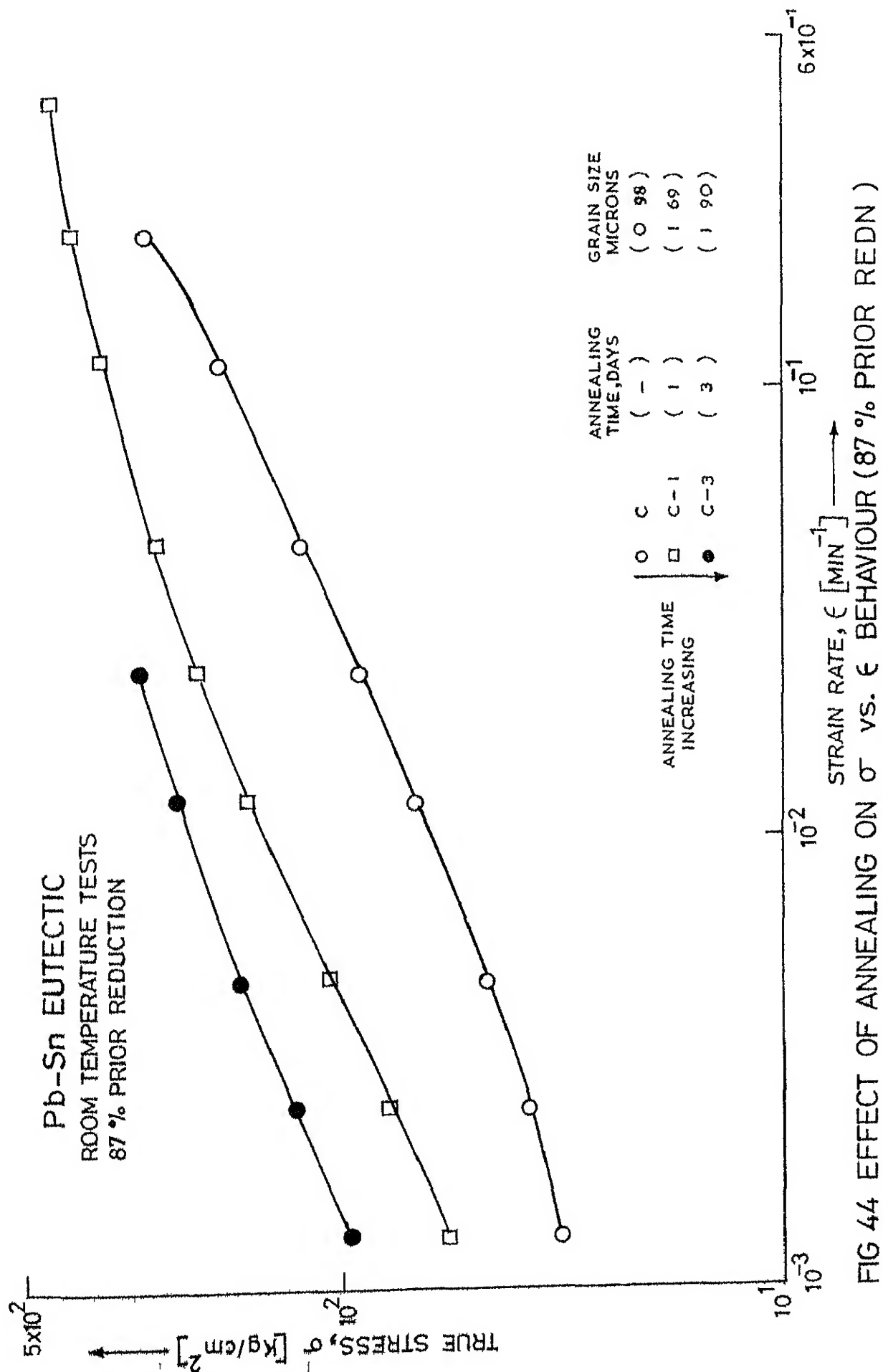


FIG 43 EFFECT OF ANNEALING ON  $\sigma$  vs  $\dot{\epsilon}$  BEHAVIOUR (73% PRIOR REDN)





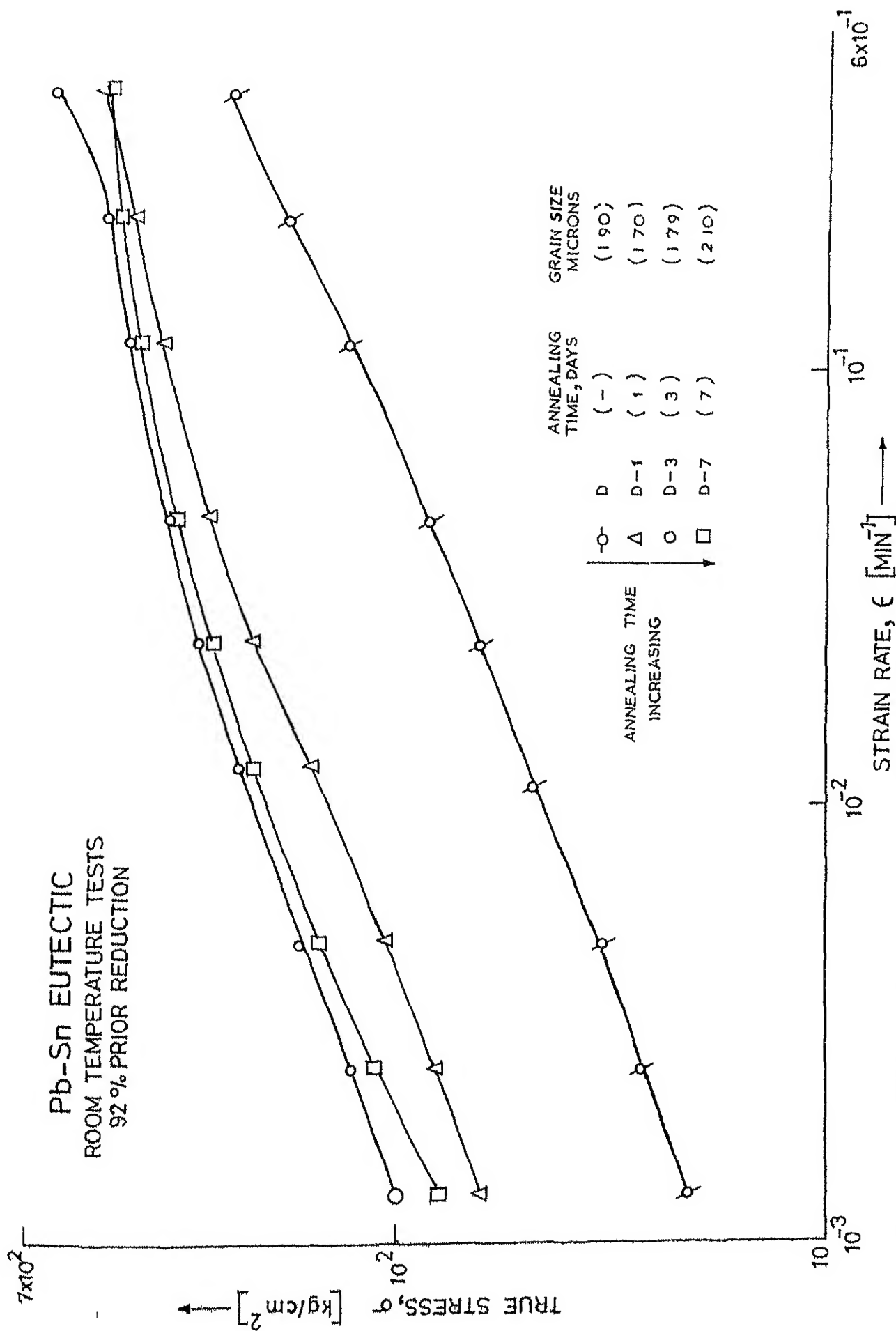


FIG 45 EFFECT OF ANNEALING ON  $\sigma$  vs  $\dot{\epsilon}$  BEHAVIOR (92% PRIOR REDUCTION)

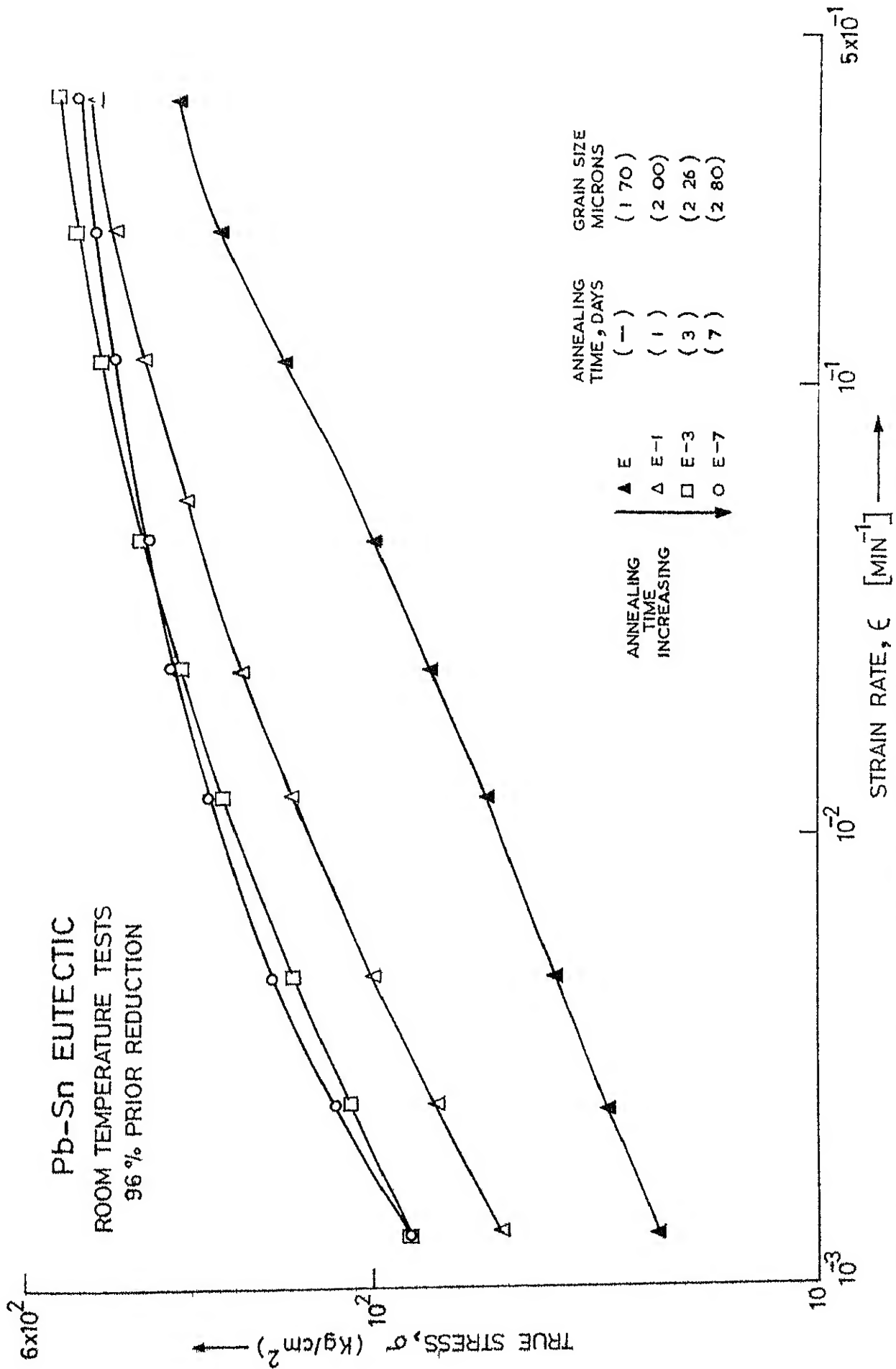


FIG.46 EFFECT OF ANNEALING ON  $\sigma$  vs  $\dot{\epsilon}$  BEHAVIOUR (96 % PRIOR REDUCTION)

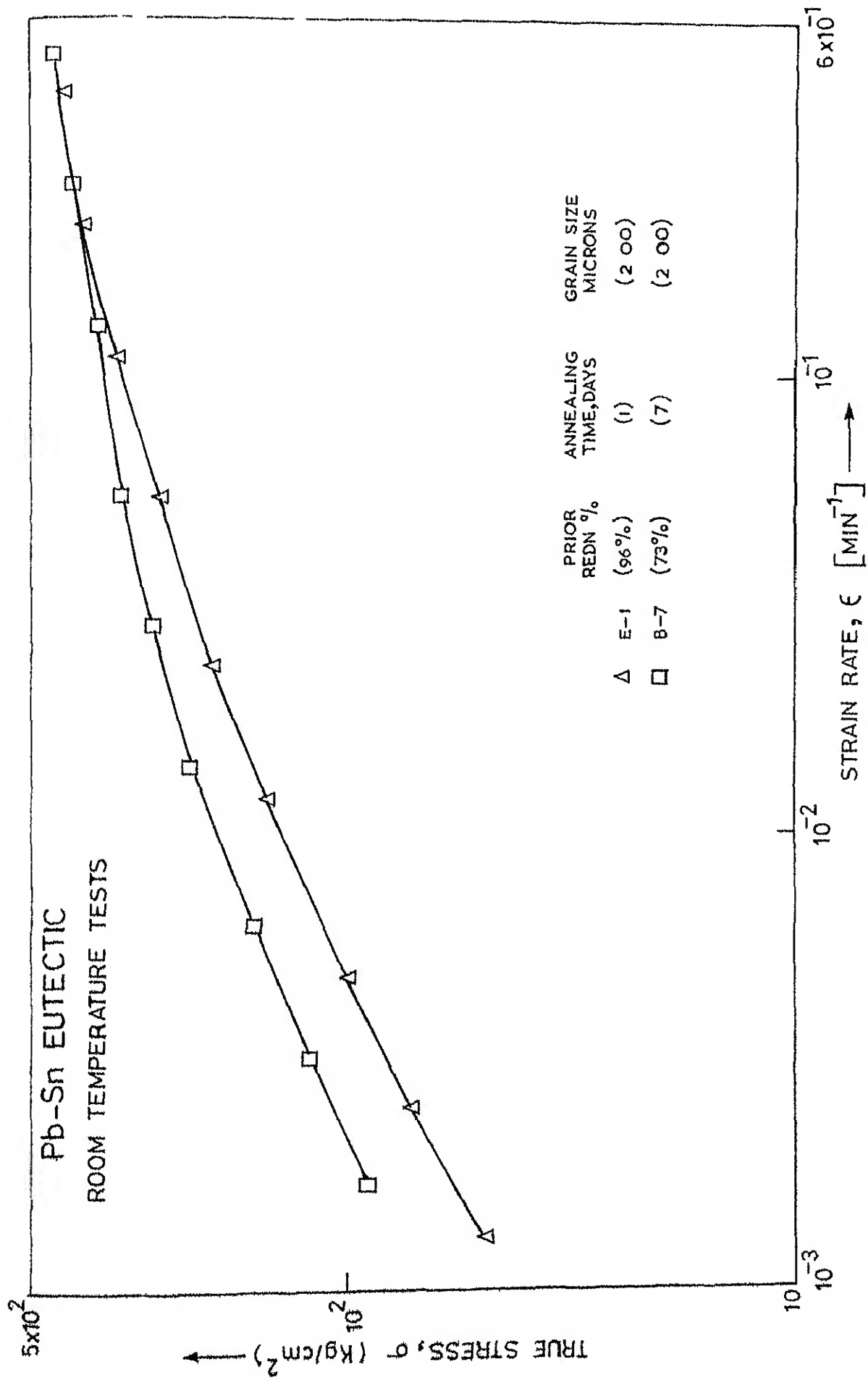


FIG 47  $\sigma$  vs  $\dot{\epsilon}$  BEHAVIOUR OF SAME GRAIN SIZED MATERIAL PROCESSED DIFFERENTLY

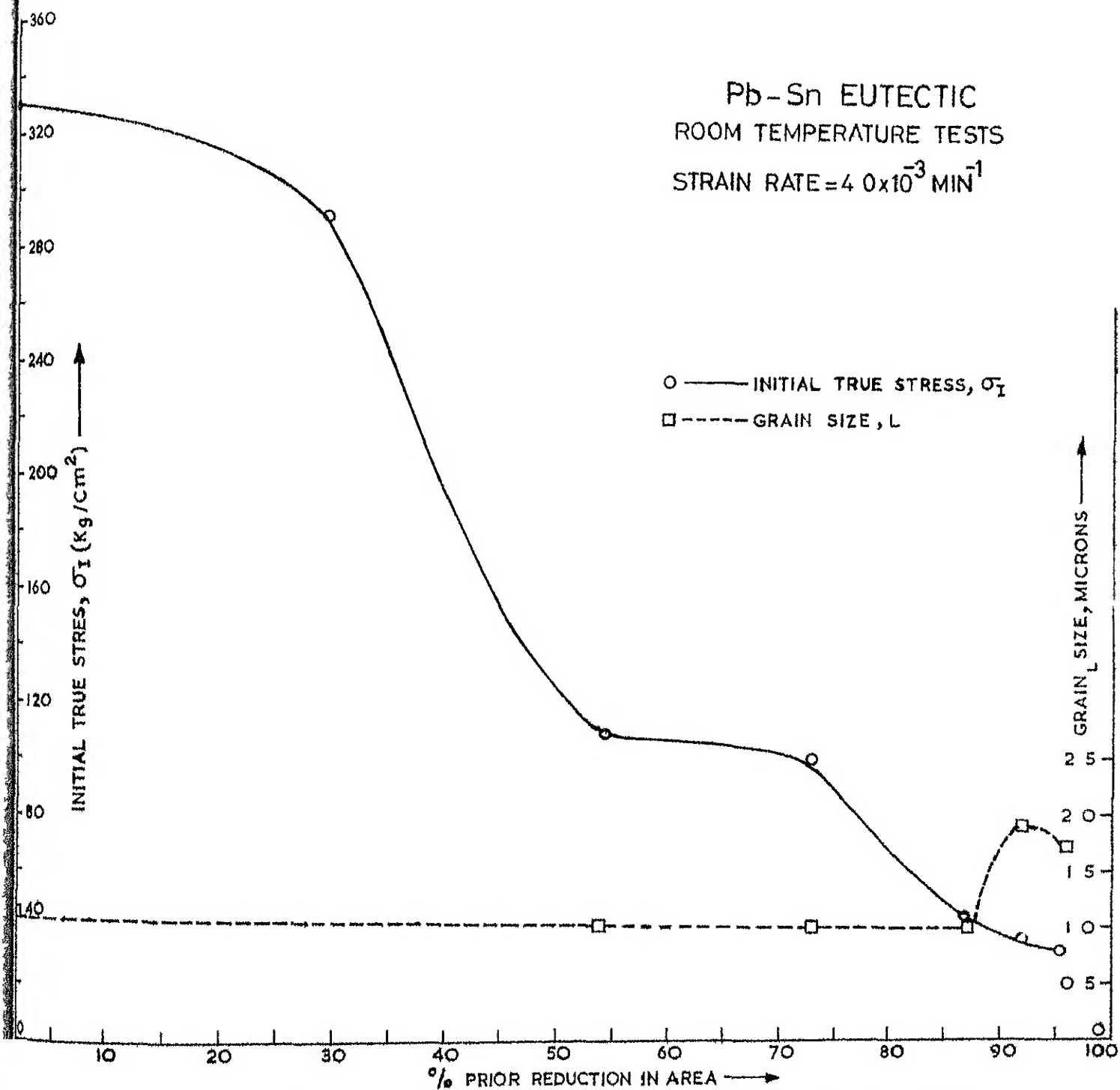


FIG 48 INITIAL TRUE STRESS AND GRAIN SIZE vs PRIOR REDUCTION

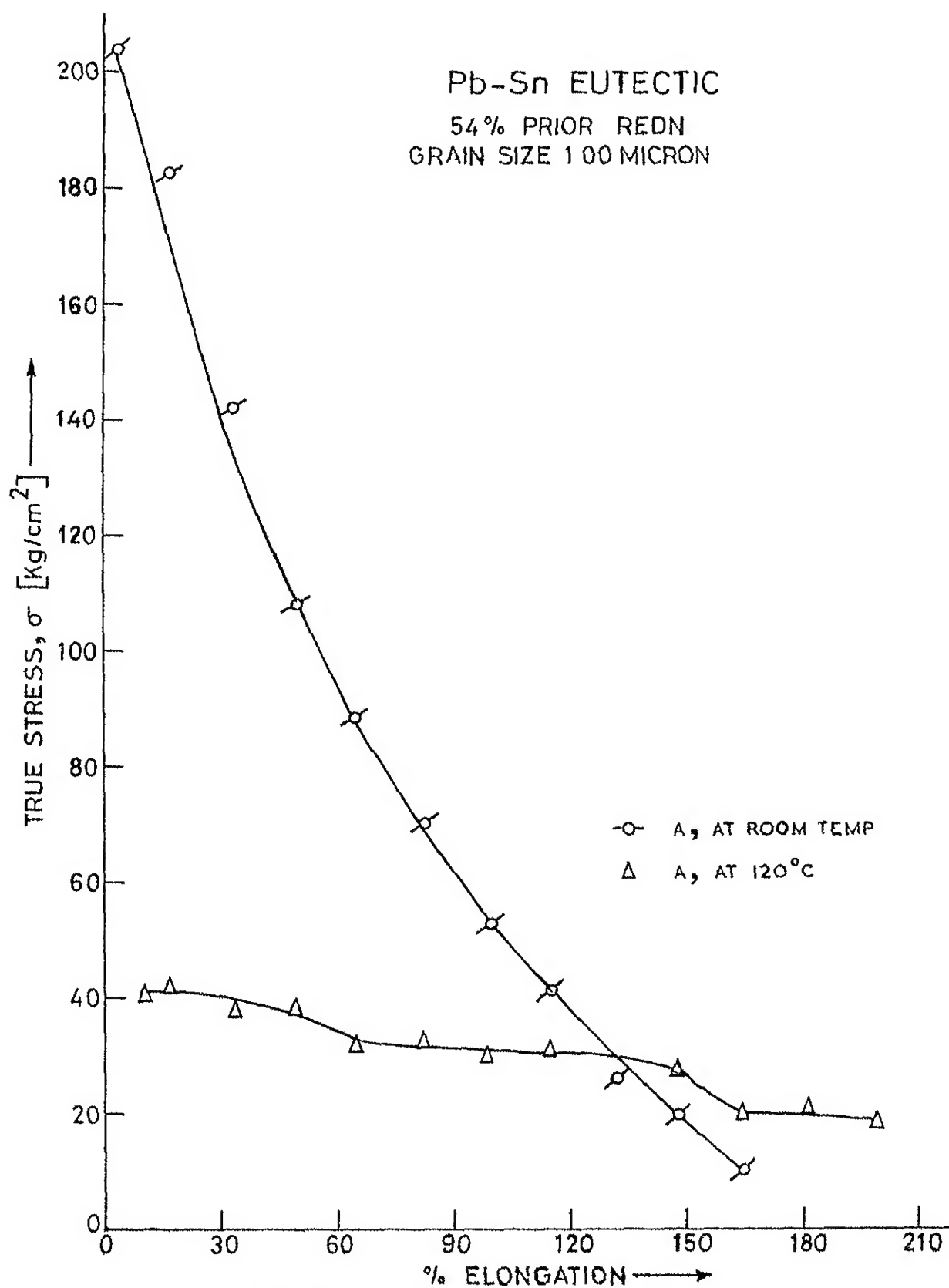


FIG 49 EFFECT OF TEST TEMPERATURE ON  $\sigma$  vs ELONG BEHAVIOUR (54% PRIOR REDN.)

Pb-Sn EUTECTIC  
ROOM TEMPERATURE TESTS  
92% PRIOR REDN

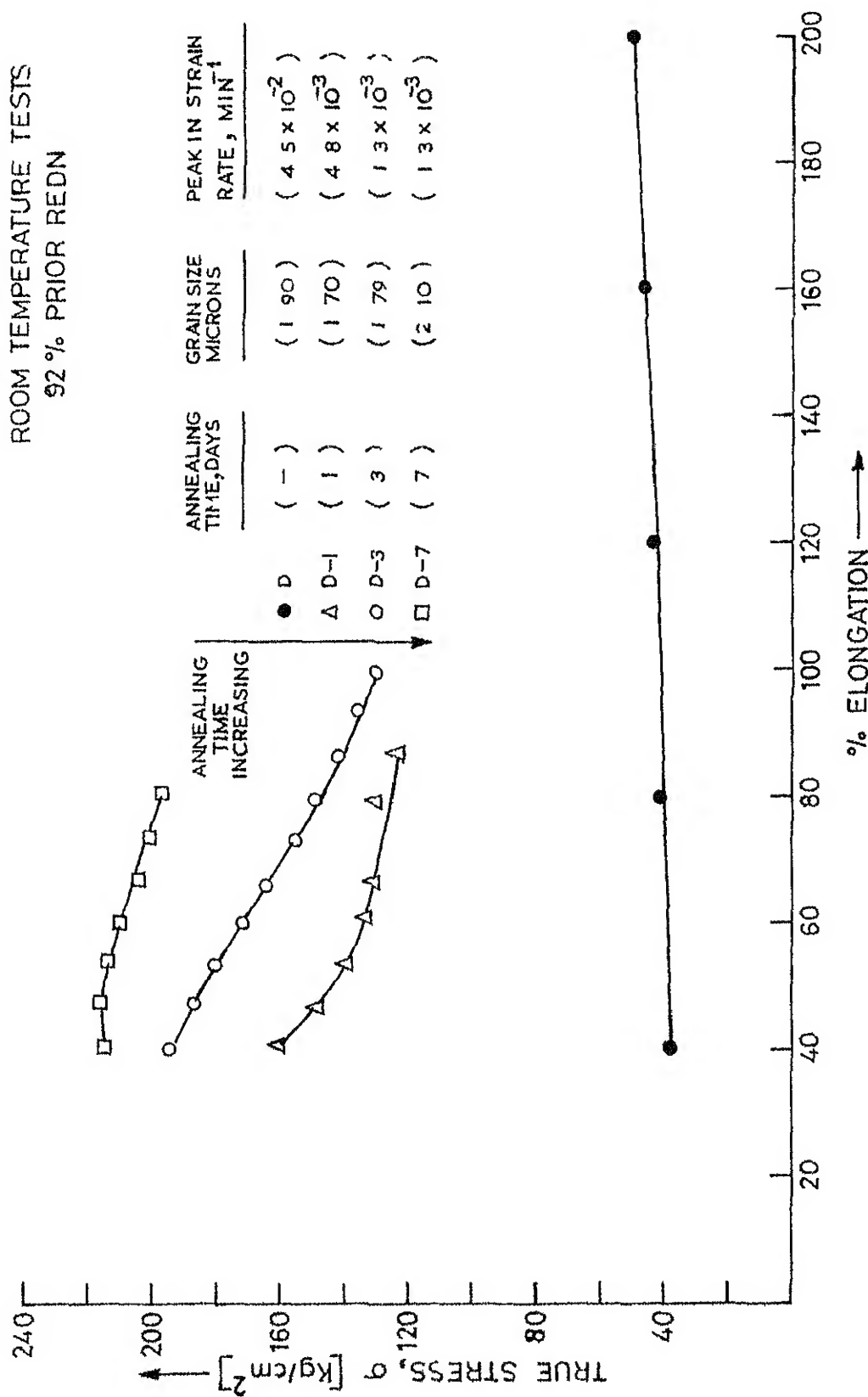


FIG 50 EFFECT OF ANNEALING ON  $\sigma$  vs % ELONGATION BEHAVIOUR  
(92% PRIOR REDUCTION)

## APPENDIX 1

MATERIALS

Materials were obtained from American Smelting and Refining Company, Central Research Lab., South Plainfield, New Jersey 07080, U.S.A. Lead was 99.99+%, Grade B-58. This was in fine granular form. This was vacuum melted to get big enough chunks to facilitate air melting for making the alloy. Spectrographic analysis of Lead indicated following impurities in p.p.m.

Sb, Tl, Mn, Sn, Cr, Ni, Bi, Ca, In and Zn : N.D. (not detected)

Mg, Si, Fe, Cu = 1 p.p.m.

Al 5, Cd = 5, Ag 1.

Tin was 99.99% purity and obtained from the Semi-Alloys Inc., U.S.A.

PHYSICAL DATA<sup>85</sup>

## (a) Metals

	<u>TIN</u>	<u>LEAD</u>
Specific Gravity	7.31 gm/cm <sup>3</sup>	11.34 gm/cm <sup>3</sup>
Melting Point	232°0	327°0
Boiling Point	2260°0	1620°0
Specific Heat	0.0536	0.0297

## (b) Eutectic Alloy

Composition: Pb - 61.9 wt.% Sn

Pb - slightly greater than 70 at.% Sn.



Volume fraction of Tin = 0.71

M.P. of eutectic = 183°C.

Solid Solubility of Sn in Pb at R.T.	= 1 wt.% Sn.
Solid Solubility of Sn in Pb at 120°C	= 6 wt.% Sn.
Solid Solubility of Sn in Pb at 183°C	= 19.2 wt.% Sn
Solid Solubility of Pb in Sn at R.T.	= Nil
Solid Solubility of Pb in Sn at 120°C	= Nil
Solid Solubility of Pb in Sn at 183°C	= 2.5 wt.% Pb

#### DIMENSIONS OF SAMPLES

Round specimen (A AND B) had a gage length of 1", and dia of gage section 0.16". It was a standard specimen specified by Instron manual.

The wire specimens (C-E) were made such that gage length was 4 x Dia. and grip sections on each side were nearly equal to the gage length.

## APPENDIX 2

MODIFICATION OF LINEAR INTERCEPT METHOD<sup>13</sup>

A two phase material will have microstructure described by either of the two following cases :

- (a) A two phase system of particles ( $\alpha$ ) embedded in a matrix ( $\beta$ ) in which the particles do not touch each other.
- (b) A two phase system of particles ( $\alpha$ ) embedded in a matrix ( $\beta$ ) in which some of the particles are touching one another ( $\alpha - \alpha$ ).

For case (a), the grain size or mean intercept length is given by

$$L = \frac{(V)_{\alpha}}{N} = \frac{2(V)_{\alpha}}{P}$$

where,  $(V)_{\alpha}$  = Volume fraction of  $\alpha$ . This value is frequently obtained by point count.

$N$  = Number of intersections of grains per unit length of a random test line.

$P$  = Number of intersections of grain boundary traces per unit length of test line.

In the case of Pb-Sn eutectic  $(V)_{\text{TIN}} = 0.71$ .

For the case (b), the grain size or mean intercept length is given by

$$L = \frac{2(V)_{\alpha}}{(P)_{\alpha-\beta} + 2(P)_{\alpha-\alpha}}$$

where  $\alpha-\beta$  refers to interface between  $\alpha$  and  $\beta$  .

$\alpha-\alpha$  refers to interface between  $\alpha$  and  $\alpha$  .

The values of  $(P)_{\alpha-\beta}$  and  $(P)_{\alpha-\alpha}$  are counted simultaneously along the same random test lines.

#### ADDITIONAL SAMPLES

Two additional samples were also studied.

They are :

<u>Identification</u>	<u>Prior Reduction,%</u>	<u>Dia.after Swaging</u>
ALPHA	29.5%	0.42"
BETA	42.3%	0.38"

## APPENDIX 3

PRECISION OF LINEAR INTERCEPT METHOD<sup>86</sup>

If  $x_1, x_2, \dots, x_n$  are the  $n$  determinations of the number of intersections, then the number of measurements necessary to provide a 65% probability that the error of the mean will not exceed  $\pm 1\%$  is given by

$$n_{65} = V_x \text{ or Variance}$$

And, the number of measurements necessary to provide a 95% probability that the error of the mean will not exceed  $\pm 1\%$  is given by

$$n_{95} = 4V_x$$

Using standard error of the mean  $S_{\bar{x}} = \left(\frac{V_x}{n}\right)^{\frac{1}{2}}$  as the measure of precision, according to statistical theory, there is a 65% probability that the mean  $\bar{x}$  will fall between the limits  $\bar{x} \pm S_{\bar{x}}$  and a 95% probability that the mean will fall in the range  $\bar{x} \pm 2S_{\bar{x}}$ . A sample calculation follows.

$$\text{Mean, } \bar{x} = 85$$

$$\text{Variance, } V_x = \frac{(x - \bar{x})^2}{n-1} = \frac{10}{9} = 1.1$$

$$\text{The standard deviation} = S_x = V_x^{\frac{1}{2}} = \pm 1.05$$

$$\text{The standard error of the mean} = S_{\bar{x}} = \frac{S_x}{(n)^{\frac{1}{2}}} = \pm 0.332$$

Table A-3.1

Count Number	Number of Intersections	$(x-\bar{x})^2$
1	86	1
2	84	1
3	85	0
4	86	1
5	83	4
6	86	1
7	86	1
8	85	0
9	84	1
10	85	0
SUM	850	10

This tells that the number of measurements necessary to provide a 95% probability that the error of the mean will not exceed  $\pm 1\%$  is  $4 \times 1.1 = 4.4$  or 5 counts.

This also tells that there is 95% probability that the mean  $\bar{x}$  will fall between the limits  $\bar{x} \pm 0.66$ . From this, error in grain size can be calculated as follows.

Grain size corresponding to mean  $\bar{x} = 85$

$$L = \frac{32.6}{2 \times 1760 \times 85} = 1.09 \text{ microns}$$

Grain size corresponding to maximum variation in  $x$  on the positive side, i.e.  $x = 85.66$ ,

$$L_{\min.} = \frac{32.6}{2 \times 1760 \times 85.66} = 1.07 \text{ microns}$$

Grain size corresponding to minimum variation in  $x$  on the negative side, i.e.,  $x = 84.34$ ,

$$L_{\max.} = \frac{32.6}{2 \times 1760 \times 84.34} = 1.10$$

Therefore, using 5 counts each time gives a 95% probability that the grain size lies between

$$1.08 \quad L \quad 1.10 \text{ microns}$$

$$\text{Or, \% error from the mean} = \frac{0.01 \times 100}{1.09}$$

$$= 0.917\%.$$

# REFERENCES

1. D.H. Avery and W.A. Backofen: Trans. ASM, 58 (1965), 551.
2. R.B. Jones and R.H. Johnson: *ibid*, 59 (1966), 356.
3. D.L. Holt and W.A. Backofen: *ibid*, 59 (1966), 755.
4. T.H. Alden: Acta Met., 15 (1967), 469.
5. C.M. Packer and O.D. Sherby: Trans. ASM, 60 (1967), 21.
6. C.M. Packer, R.H. Johnson and O.D. Sherby: Trans. AIME-TMS, 242 (1968), 2485.
7. P. Chaudhari: Acta Met., 15 (1967), 1777.
8. H.W. Hayden, R.C. Gibson, H.F. Merrick and J.H. Brophy: Trans. ASM, 60 (1967), 3.
9. W.A. Backofen, F.J. Azzarto, G.S. Murty and S.W. Zehr: ASM, Seminar on Ductility (1968), 279.
10. W.A. Backofen, I.R. Turner and D.H. Avery: Trans. ASM, 57 (1964), 980.
11. R.C. Gifkins: J. Inst. Metals, 95 (1967), 373.
12. J.J. Jonas, C.M. Sellars, and W.J. McG. Tegart: Met. Review (1969), 14 (130), 1.
13. Ultrafine-Grain Metals: Editors: John J. Burke and Volker Weiss, Proceedings of the 16th Sagamore Army Materials Research Conference, Syracuse University Press, First Edition (1970).
14. R.H. Johnson: Metals and Materials and Met. Reviews, Vol.4, Sept. 1970, p.115.
15. H.E. Oline and T.H. Alden: "Rate Sensitive Deformation in Tin-Lead Alloys", Trans. AIME 239 (1967) 710.
16. Lee, D., "Structural Changes During Superplastic Deformation", Met. Trans.1 (1970), 309.
17. E.E. Underwood, "A Review of Superplasticity and Related Phenomenon", J. Metals, 14 (1962), 914.



18. W.A. Backofen, I.R. Turner and D.H. Avery, "Superplasticity in an Al-Zn Alloy", Trans. ASM Quart., 57 (1964), 980.
19. G.J. Davies, J.W. Edington, C.P. Outler and K.A. Padmanabhan, "Superplasticity - A Review", J. of Mat.Sc., 1970, No.12, Vol.5, 1091.
20. C.E. Pearson: J. Inst. Metals, 54 (1934) 111.
21. G. Doyle: S.B.Thesis, M.I.T. (1966).
22. D.H. Avery and J.M. Stuart, "The Role of Surfaces in Superplasticity in Near-Eutectic Lead-Tin Alloy", Surfaces and Interfaces, Vol.II (1968), Syracuse University Press, N.Y.
23. J.W. Aldrich and D.H. Avery: "Alternating Strain Behaviour of Superplastic Lead-Tin Eutectic", 16th Sagamore Army Materials Research Conference.
24. P.J. Martin and W.A. Backofen, "Superplasticity in Electro-Plated Composites of Lead and Tin": Trans. ASM 60 (1967), 352.
25. R.A. Saller and J.L. Dunoon, "Stamping Experiments with Tin-Lead and Other Superplastic Alloys", J. Inst. Metals, Vol.99 (1971), 173.
26. D. Lee and W.A. Backofen, Trans. TMS-AIME, 239 (1967), 1034.
27. D.L. Holt: *ibid*, 242 (1968), 25.
28. E.W. Hart, "Theory of the Tensile Test", ACTA Met., 15 (1967), 351.
29. A. Karim, D.L. Holt and W.A. Backofen, TMS-AIME, 245 (1969), 1131.
30. O. Herring, J. Appl. Phys. 21 (1950), 437.
31. R.L. Coble, *ibid*, 34 (1963), 1679.
32. F.R.N. Nabarro, Proc. Conf. on Strength of Solids, Phys. Soc. of London, Cambridge (1948), 75.
33. I.M. Lifshitz, Soviet Physics JETP 17 (1963), 909.
34. E.O. Bingham, Scientific Paper No.278, U.S. Bureau of Standards.
35. H.E. Cline and T.H. Alden, "Superplasticity in Lead-Tin Alloys", TMS-AIME 239 (1967), 1034.

36. D.L.Holt: TMS-AIME, 242 (1968), 740.
37. A. Nadai and M.J.Manjoine; J.Appl.Mech., 8 (1941), A77.
38. D.S. Fields, Jr. and W.A. Backofen; Trans. ASM, 51 (1959), 946.
39. O. Rossard; Rev. Met., 63 (1966), 225.
40. J.D. Campbell; J. Mech. Phys. Sol., 15 (1967), 359.
41. E. Orowan; Reports Progr. Physics, 12 (1948-49), 185.
42. A.H.Cottrell and V. Aytakin; J. Inst. Metals, 77 (1950), 389.
43. D. McLean: "Mechanical Properties of Metals", 1962, p.295: N.Y. and London, John Wiley.
44. T.H.Alden: ACTA Met. 15 (1967), 469.
45. K. Nuttall and R.B.Nicholson: Phil.Mag., 17 (1968), 1087.
46. R.O. Cook and N.R. Risebrough: Scripta. Met. 2 (1968), 487.
47. H.Naziri and R. Pearce: J. Inst. Metals, 97 (1969), 326.
48. Idem: Scripta Met., 3 (1969), 807.
49. Idem; Ibid, 3 (1969), 811.
50. Idem, J. Inst. Metals, 98 (1970), 71.
51. H.W. Hayden and J.H.Brophy: Trans. ASM, 61 (1968), 542.
52. D.A. Wood Ford; Trans. ASM, 62 (1969), 291.
53. T.H.Alden: J. Aust.Inst.Met., 14 (1969), 207.
54. C.J.Smithells: "Metals Reference Book" 4th Edition (Butterworths, London 1967), pp.644-645.
55. W. Lange and D. Bergner: Phys. Stat. Sol., 2 (1962), 1410.
56. B. Okkerse: ACTA Met. 2 (1954), 551.
57. C.H.M.Jenkins: J. Inst.Metals, 40 (1928), 21.
58. W.B.Morrison: TMS-AIME, 242 (1968), 2221.
59. S.W.Zehr and W.A. Backofen: Trans. ASM, 61 (1968), 300.
60. J.Weertman and J.E.Breent Trans. Am.Inst.Min.Met.Eng. 1955, 203, 1230.

61. A. Ball and M.M. Hutchinson: Metal Sci.J., 3 (1969), 1.
62. H. Gleiter, E. Hornbogen and G. Baro, ACTA Met., 16 (1968), 1053.
63. C.M.Packer, R.H. Johnson and O.D.Sherby: Trans. MS AIME, 242 (1968), 2485.
64. F.Hargreaves: J. Inst. Metals, 1928, 39, 301.
65. Idem, ibid, 1927, 37, 103.
66. F. Hargreaves and R.J.Hills: ibid (1928), 40, 41.
67. C.M.Packer and O.D.Sherby: Trans. ASM, 1967, 60, 21.
68. G. Cook: J. Inst. Metals, 1934, 40, 134.
69. R.B.Jones and R.H.Johnson: Trans. ASM, 1966, 59, 356.
70. R.H.Johnson, R.B.Jones and E.C.Sykes: Unpublished work.
71. J. Weertman: J. Appl. Physics, 1957, 28, 362.
72. R.N. Stevens: Met. Rev., 1966, 11 (108), 129.
73. E.Orowan: Progress in Physics, 1948-49, 12, 185.
74. R.C.Gifkins: J. Inst. Metals, 1967, 95, 373.
75. R.C.Gifkins and K.U.Snowden: TMS-AIME, 1967, 239, 910.
76. J.E. Harris: TMS-AIME, 1965, 233, 1509.
77. Y. Iehida and D. McLean: Metal Sci.J., 1967, 1, 171.
78. C.P.Outler and J.W.Edington: (To be published).
79. B. Burton: Scripta. Met. Vol.5, No.8, p.669.
80. J.J. Jonas, C.M. Sellars and W.J. McGe Tegart: Met. Rev., 1969, 14 (130), 1.
81. R.H.Johnson: Design Engineering, March 1969, p.33.
82. T.Y.M. Al-Naib and J.C.Duncan: Internat.J. Mech. Sci., 12 (1970), 463.
83. B.B.Hundy, "Plasticity and Superplasticity", Inst. of Metallurgists Review Course, Series 2, No.3 (1969), p.73.
84. S.P.Rawal: M.Tech.Thesis, 1969, I.I.T. Kanpur, India.

85. Metals Reference Book, Vol.1, Smithells, III Edition, Washington Butterworths (19962).
86. M. Cohen and R.T. Howard, Trans. AIME, 1947, Vol.172, p.413.
87. B.M.Watts and M.J.Stowell, J.Mat.Sc. 6 (1971), p.228-237.
88. J.L.Robbins, O.C. Shepard and O.D.Sherby, J.I.S.I., 1964, 202, 804.
89. E.A. Chojnowski and W.J.McG Tegart, Metal Sci.J., 1968, 2, 14.

Thesis

630

669.4

C361

Chandan,

Relation between super-  
plasticity and prior thermo-  
mechanical treatment in lead  
tin eutectic.